

1971

Losses in trapped-mode resonators

David Maurice Morton
Iowa State University

Follow this and additional works at: <https://lib.dr.iastate.edu/rtd>

 Part of the [Electrical and Electronics Commons](#)

Recommended Citation

Morton, David Maurice, "Losses in trapped-mode resonators " (1971). *Retrospective Theses and Dissertations*. 4491.
<https://lib.dr.iastate.edu/rtd/4491>

This Dissertation is brought to you for free and open access by the Iowa State University Capstones, Theses and Dissertations at Iowa State University Digital Repository. It has been accepted for inclusion in Retrospective Theses and Dissertations by an authorized administrator of Iowa State University Digital Repository. For more information, please contact digirep@iastate.edu.

72-5239

MORTON, David Maurice, 1941-
LOSSES IN TRAPPED-MODE RESONATORS.

Iowa State University, Ph.D., 1971
Engineering, electrical

University Microfilms, A XEROX Company, Ann Arbor, Michigan

Losses in trapped-mode resonators

by

David Maurice Morton

A Dissertation Submitted to the
Graduate Faculty in Partial Fulfillment of
The Requirements for the Degree of
DOCTOR OF PHILOSOPHY

Major Subject: Electrical Engineering

Approved:

Signature was redacted for privacy.

In Charge of Major Work

Signature was redacted for privacy.

For the Major Department

Signature was redacted for privacy.

For the Graduate College

Iowa State University
Ames, Iowa

1971

TABLE OF CONTENTS

	Page
LIST OF SYMBOLS	iv
I. INTRODUCTION	1
A. General Comments	1
B. Applications of Trapped-mode Resonators	3
C. Statement of the Problem	5
II. ANALYSIS OF TRAPPED-MODE STRUCTURES: CLOSED-FORM SOLUTIONS	8
A. Introductory Comments	8
B. Rectangular Geometry: Quasi-dominant Mode	10
C. Cylindrical Geometry: Circulating Electric Field Mode	18
III. ANALYSIS OF TRAPPED-MODE STRUCTURES: APPROXIMATE SOLUTIONS	25
A. Introductory Comments	25
B. Variational Formulation	26
C. Finite-difference Formulation	37
IV. EXPERIMENTAL INVESTIGATION	40
A. Experimental Resonator Design	40
B. Measurement Technique	45
V. COMPARISON OF THEORETICAL AND EXPERIMENTAL DATA	50
VI. SUMMARY AND CONCLUSION	57
VII. LITERATURE CITED	60
VIII. ACKNOWLEDGMENTS	63
IX. APPENDIX A: VARIATIONAL FORMULATION EXAMPLE	64

	Page
X. APPENDIX B: CONSTRUCTION OF THE FINITE-DIFFERENCE ANALYSIS PROGRAM	68
XI. APPENDIX C: FINITE-DIFFERENCE ANALYSIS PROGRAM	75

LIST OF SYMBOLS

A	-	matrix
\underline{E}	-	electric field intensity
\underline{H}	-	magnetic field intensity
I	-	identity matrix
\underline{J}	-	electric current density
J_i	-	i th order Bessel function of the first kind
\underline{J}_s	-	electric surface current density
K_i	-	i th order modified Bessel function of the second kind
L	-	continuous linear operator
L_d	-	discrete linear operator
\underline{M}	-	magnetic current density
\underline{M}_s	-	magnetic surface current density
P_d	-	power dissipated
Q	-	quality factor
R	-	relaxation formula
R_s	-	surface resistance coefficient
S	-	boundary surface
W	-	energy
\overline{W}_e	-	time-averaged electric field energy
\overline{W}_m	-	time-averaged magnetic field energy
Z_s	-	surface impedance
a	-	physical dimension
b	-	physical dimension

c	-	physical dimension
d	-	physical dimension
$d\mathbf{s}$	-	differential (vector) surface element
dv	-	differential volume element
\underline{e}	-	electric field intensity
f_r	-	resonant frequency
h	-	expansion coefficient
j	-	square root of -1
k	-	expansion coefficient
\underline{n}	-	unit normal vector
ϕ	-	variational parameter
r	-	cylindrical coordinate
s	-	general surface
t	-	physical dimension
v	-	volume
x	-	rectangular coordinate
y	-	rectangular coordinate
z	-	rectangular or cylindrical coordinate
β	-	accelerating factor
δ^i	-	ith variation
ϵ	-	permittivity
ϵ_0	-	permittivity of free space
ϵ_r	-	relative permittivity
κ	-	wave number in the direction of evanescence in cutoff waveguide
λ	-	eigenvalue

μ	-	permeability
μ_0	-	permeability of free space
ϕ	-	continuous eigenfunction
ϕ_d	-	discrete eigenfunction
ϕ	-	cylindrical coordinate
ω	-	angular frequency
ω_r	-	resonant angular frequency

I. INTRODUCTION

A. General Comments

Resonant circuits are of great importance in applications such as oscillator circuits, tuned amplifiers, frequency filter networks, wavemeters for measuring frequency, etc., at frequencies ranging from a few Hertz to optical frequencies. Electromagnetic resonators can assume several different physical forms, depending largely upon the frequency of operation of the particular circuit in which the resonator is used.

Electromagnetic resonators are classified on the basis of their characteristics at and near resonance--the condition when the time-averaged electric- and magnetic-field energies are equal. The characterization near the frequency at which resonance occurs is based on the frequency of resonance and a term called the quality factor or Q. The quality factor is related to the ratio of the energy stored within the resonator to the power dissipated in the resonator.

At lower frequencies (below about 100 MHz) electromagnetic resonators are generally realized from conventional lumped inductance and capacitance elements. In this frequency range, wavelengths are generally long compared to the physical dimensions of the components.

At higher frequencies where wavelength effects must be considered (approximately 100 to 1000 MHz), transmission-line sections with open-circuit or short-circuit terminations are used as electromagnetic resonators with the specific configuration used depending upon the specific application. The behavior of these transmission-line resonators

is not unlike that of the corresponding low-frequency lumped-element resonators. Because of the distributed parameter nature of transmission-lines, however, these resonators will exhibit a multiplicity of resonances which must not be ignored in that undesired spurious responses may result.

At frequencies higher than about 1000 MHz, the value of the quality factor for transmission-line resonators deteriorates and metallic enclosures, or cavities, are used instead. The electric and magnetic fields are contained within the structure and are supported by electric charge distributions on and electric currents flowing in the walls. For cavities, the frequency of resonance is determined primarily by the physical characteristics of the structure (size, shape, dielectric material) and the electromagnetic field at resonance. As is true for transmission-line resonators, more than one resonant frequency is possible. The quality factor is dependent upon similar factors and, additionally, the material from which the resonator is constructed. A detailed examination of the electromagnetic field pattern for a particular mode of interest will indicate that the resonator boundary may be modified somewhat without greatly affecting the charge and current distributions there.

A trapped-mode resonator is a microwave resonator configuration which is able to constrain an electromagnetic field despite physical openings in its boundary surface. By the appropriate choice of the shape of the openings, it is possible to suppress certain of the undesired resonances which would exist in a conventional solid wall resonator while having very little effect upon the desired resonance.

B. Applications of Trapped-Mode Resonators

The low-loss characterization of a trapped mode resonator plus the inherent rejection of certain resonances make its utilization as a microwave circuit element an obvious application. Post, Potter, and Risser (24) have discussed the use of a circular trapped-mode resonator for microwave filter applications.

Matthaei and Weller (20) constructed a circular trapped-mode band-pass filter and conducted a testing program to examine the spurious responses of their device. They report excellent rejection of signals in the stop-band of a four-resonator filter with two of the resonators being trapped-mode sections. The trapped-mode resonators were of cylindrical geometry with grooves about the circumference of the cylindrical surface. Thus, only a circumferential conduction current could exist and many of the unwanted modes which would otherwise be present were suppressed.

In a companion article to the one cited immediately above, Schiffman, Matthaei, and Young (29) reported on a rectangular geometry trapped-mode filter. The operation of the resonators in filter was essentially that of resonators constructed of conventional rectangular waveguide except that in place of shorting plates, metallic septa were placed to form the mode-trapping boundaries. The absence of spurious pass-bands over a wide frequency range is reported for this configuration, also.

Risser (27) constructed and tested circular geometry trapped-mode band-pass filters consisting of three and five trapped-mode resonators.

His discussion gives details of alignment as required to provide the desired pass-band response characteristic. He also provides data describing the performance of the realized filters.

The design and analysis of a tunable cylindrical geometry trapped-mode resonator was reported by Morton (23). By changing the position of the conducting rings at the circular boundary in a particular manner, the resonant frequency of the trapped-mode section could be adjusted. Thus, a tunable resonator with constant axial length was realized, permitting the construction of a filter which does not exhibit a change in size as it is aligned. Quality factor measurements indicated that the resonator tested had low losses throughout its tuning range.

Robinson¹ conducted tests of rectangular and circular open-wall cavities and reported the resonant frequency and quality factor data. Included was data relating the decrease of resonator quality factor to the deviation from parallel of the conductors on the cylindrical boundary of trapped-mode resonators.

Potter (25) analyzes a circular geometry trapped-mode resonator as a periodic structure and discusses its utility as a sampling cavity, perhaps in a refractometer such as that realized by Vetter and Thompson (31). Because of the high degree of openness of Potter's trapped-mode resonator it is suggested that it might provide more rapid flushing than would the particular resonator design used by Vetter and Thompson

¹Robinson, L. A. Palo Alto, Calif., Experimental Results. Private communication. 1966.

and thereby make the refractometer more sensitive to short-term variations in refractive index.

C. Statement of the Problem

It is the purpose of this thesis to investigate specialized analytical techniques for the calculation of conductor losses in trapped-mode resonators. Of particular interest are those configurations where an exact solution of the loss-free problem is not feasible in that there are two regions for solution which must be joined at a surface which may not be explicitly determined in a mathematical sense. The specifications of resonant frequency and quality factor are of great utility for engineering applications of resonators such as these.

Several researchers have reported work which is somewhat related to the problem at hand. Marcatili (19) solved the problem of the heat loss in metallic waveguide walls with grooves of circular cross section. His solution applies to circular grooves with a diameter which is small compared to the wavelength at the frequency of operation and large compared to the skin depth of the wall material.

Morrison (22) solves a similar problem by making a quasi-static approximation at the grooved surface and using conformal mapping to solve Laplace's equation for the resulting two dimensional problem. His solution applies to grooves similar to those considered by Marcatili and achieves the similar result that the attenuation of a helix waveguide is higher than that of a comparable smooth wall guide.

By means of a modal expansion, the problem of finding the attenuation and propagation factor of spaced-disc circular waveguide is considered by Gent (11). His formulation yields the result that the attenuation of a spaced-disc guide (a structure not unlike the circular walls of a trapped-mode resonator) is lower than that of a solid wall guide. Although his problem is not identical to that of Marcatili or Morrison, he acknowledges the apparent contradiction without resolving it.

Bryant (6) considers the propagation in corrugated waveguides, devoting his attention primarily to those modes which are useful in linear accelerator applications and to the corresponding aspects of the propagation constants of the guided waves.

These references are useful to the problem here only to the extent that the electromagnetic field solution developed for the waveguide situation may be extended to solve the corresponding resonator problem. As is also true for the periodic structure analysis previously mentioned, it is felt that there is a lack of flexibility in such a technique in that the formulation of the problem for reactive boundaries which possess other than simple periodicity is apt to be quite complicated.

In the following development, there are two examples of trapped-mode resonators for which the lossless problem may be solved exactly. Using the usual perturbation technique, the losses are calculated for these examples and the quality factor is shown to be greater than for the corresponding solid wall resonators. The inclusion of these specific examples is not intended to constitute a generalization that all trapped-mode resonators will exhibit quality factors which are greater than

their solid wall counterparts, but to establish that the situation is not unreasonable.

Attention is then given to the solution of those trapped-mode resonator configurations which do not yield to exact lossless electromagnetic field solutions. Two techniques are considered: solution by means of a variational formulation and by finite-difference techniques appropriate for use on a digital computer.

Finally, specific examples of the approximate techniques developed are given in detail. The result of corresponding laboratory measurements is included.

II. ANALYSIS OF TRAPPED-MODE STRUCTURES: CLOSED-FORM SOLUTIONS

A. Introductory Comments

A trapped-mode resonator may be considered to be a resonator in which the electromagnetic field is constrained by a reactive surface over part or all of the boundary. Since the physical realization of a reactive surface involves the reflection of energy by some structure, an important consideration is whether the replacement of a metallic surface with a reactive one will seriously degrade the quality factor of the resonator.

The following two examples are intended to provide some insight into this question. The first example compares a closed rectangular resonator operating in its dominant mode with a trapped-mode resonator which has a similar electromagnetic field configuration. The trapped-mode resonator is formed from the closed resonator by removing one wall and replacing it with a reactive surface which is realized by means of a cutoff waveguide. The second example compares a closed cylindrical cavity with a trapped-mode resonator which has a reactive surface replacing its cylindrical conducting surface. Again, the reactive surface is realized by means of a cutoff waveguide.

The examples are limited somewhat in that there is little, if any, practical application in an engineering sense for the particular physical configurations considered. This is due to the fact that the adjustment of the resonant frequency would be difficult. Further, the assumption of a loss free dielectric might not be practical.

The significance of these examples is that their solutions are exact within the limits imposed by the perturbation calculation used for good conductors. This approximation, which is used throughout this thesis, is well established and is documented in numerous texts (5, 13, 26). In this technique, the approximate field solution is found by assuming that there are no losses. From this solution, the electric surface current density in the conducting walls is determined and the perturbed quantity--the wall loss--is found by multiplying this current density by the surface resistance of the assumed wall material. This quantity is then integrated over the surface of the cavity to determine the power dissipated.

The quality factor is given by Harrington (13) as

$$Q = \frac{\omega W}{P_d} \quad (2.1.1)$$

Since at resonance the peak energy stored in the electric field is equal to the peak energy stored in the magnetic field it may be written that

$$W = \bar{W}_e + \bar{W}_m = 2\bar{W}_e = 2\bar{W}_m \quad (2.1.2)$$

where the overbar is used to denote the average with respect to time.

The evaluation of Equation 2.1.1 is slightly simplified if part of Equation 2.1.2 is used: Because the calculation of P_d generally involves the magnetic field intensity (evaluated at the resonator walls in order to determine the current density there), the energy storage term W will be expressed in terms of the time-averaged magnetic energy storage term \bar{W}_m . This approach simplifies the constant terms which must be manipulated

to evaluate the quality factor using Equation 2.1.1. (This approach is similar to that of Moreno (21).)

Appropriate integral expressions for \overline{W}_m and P_d are

$$W_m = \frac{1}{2} \mu \iiint_V |\underline{H}|^2 dv \quad (2.1.3)$$

and

$$P_d = R_s \iint_S |\underline{H}|^2 |d\underline{s}|. \quad (2.1.4)$$

Combining the above four equations gives

$$Q = \frac{\omega \mu \iiint_V |\underline{H}|^2 dv}{R_s \iint_S |\underline{H}|^2 |d\underline{s}|}. \quad (2.1.5)$$

Since the surface resistance is dependent upon frequency, the two examples that follow will compare losses in trapped-mode resonators to losses in closed resonators with the same resonant frequency. Thus, any change in quality factor due to change of surface resistance is not a consideration. (If comparison of quality factors is to be made over a narrow frequency range, this surface resistance change is generally negligible in that the term varies as the square root of frequency (5, 13).)

B. Rectangular Geometry: Quasi-dominant Mode

The operation of a rectangular cavity at its lowest resonant frequency (dominant mode) is the closed resonator to be considered in this example. Consider that such a resonator has all walls of similar material and has dimensions a , b , and c (all in meters and such that

$a \leq b$ and $a \leq c$) oriented along the x , y , and z coordinate axes (respectively) in a right-handed cartesian system. This situation is illustrated in Figure 2.1.

The lowest resonant frequency for such a configured resonator is well known (13) and is given by

$$f_r = \omega_r / 2\pi = \frac{1}{2}(\mu\epsilon)^{-\frac{1}{2}}(1/b^2 + 1/c^2)^{\frac{1}{2}}. \quad (2.2.1)$$

This resonant frequency corresponds to an electromagnetic field distribution which is proportional to

$$\begin{aligned} E_x &= \sin(\pi y/b)\sin(\pi z/c) \\ H_y &= (-\pi/j\omega\mu c)\sin(\pi y/b)\cos(\pi z/c) \\ H_z &= (\pi/j\omega\mu b)\cos(\pi y/b)\sin(\pi z/c) \\ E_y = E_z = H_x &= 0. \end{aligned} \quad (2.2.2)$$

The separation equation is contained in Equation 2.2.1 and is rewritten for convenience as

$$\omega_r^2 \mu_0 \epsilon_0 \epsilon_c = (\pi/b)^2 + (\pi/c)^2 \quad (2.2.3)$$

where ϵ_c is the relative permittivity of the non-magnetic dielectric contained within the volume of the resonator.

Evaluating Equation 2.1.5 using the field expressions given by Equation 2.2.2 gives the result that the quality factor for the closed dominant mode (TE_{011} mode) resonator is

$$Q_{011}^{\text{closed}} = \frac{\omega\mu}{R_s} \frac{(a/4)(b/c + c/b)}{ab/c^2 + ac/b^2 + \frac{1}{2}(b/c + c/b)}. \quad (2.2.4)$$

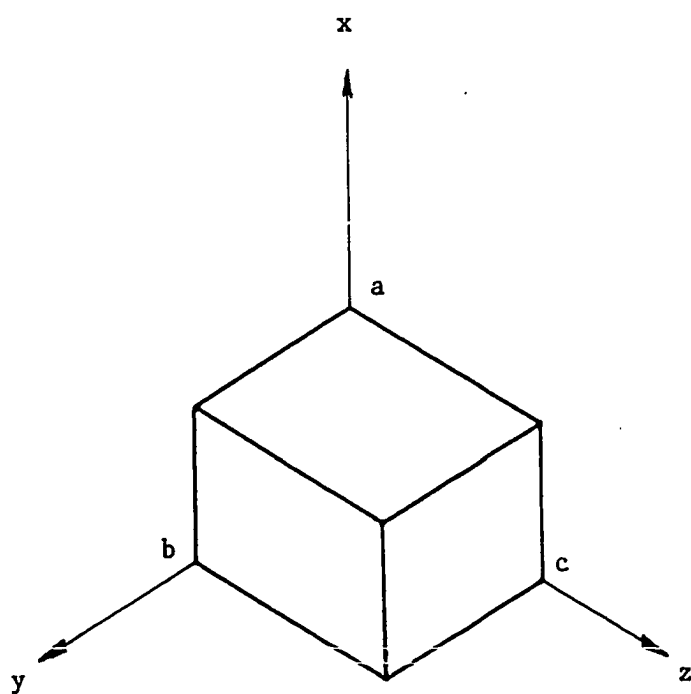


Figure 2.1. Closed rectangular resonator

In order to evaluate the losses in a rectangular resonator with part of the boundary replaced by a reactive surface, the following physical configuration is considered. The face at $z = c$ of the rectangular resonator just considered is removed and replaced by a waveguide with x - and y - dimensions equal to a and b , respectively. See Figure 2.2. In order to insure that the surface so created is reactive, the waveguide must have a cutoff frequency which is greater than f_r . This will be achieved by proper choice of the relative permittivities for the dielectrics which are in the closed cavity volume and in the interior of the waveguide. Also, the z -dimension of the dielectric must be changed to d meters in length in order that the resonant frequency be unchanged.

For the relative dielectric constant in the closed resonator being equal to ϵ_c and the relative dielectric constant in the waveguide equal to ϵ_w , the following inequality may be developed from waveguide cutoff considerations given above by using Equation 2.2.1 and an expression for the cutoff frequency (see Reference 1, 5, 13, or 26).

$$\epsilon_c / \epsilon_w > 1 + (b/c)^2 \quad (2.2.5)$$

Clearly, the condition that $\epsilon_c > \epsilon_w$ must always be satisfied.

The field solution for the region $z \geq d$ is of the form

$$\begin{aligned} E_x &= E_w \sin(\pi y/b) \exp(-\kappa z) \\ H_y &= (\kappa E_w / j\omega\mu) \sin(\pi y/b) \exp(-\kappa z) \\ H_z &= (\pi E_w / j\omega\mu b) \cos(\pi y/b) \exp(-\kappa z) \\ E_y &= E_z = H_x = 0 \end{aligned} \quad (2.2.6)$$

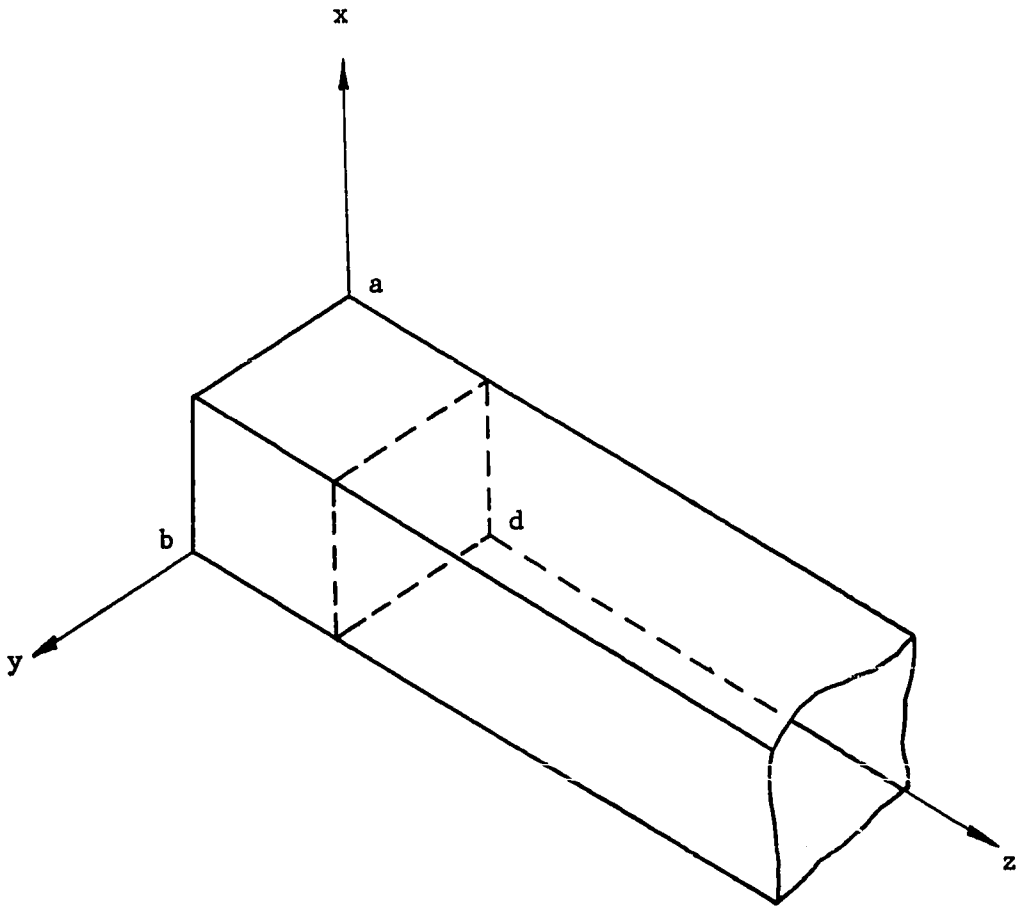


Figure 2.2. Trapped-mode rectangular resonator

where E_w is an amplitude coefficient which is to be determined.

The separation equation for this region is

$$\omega_r^2 \mu_0 \epsilon_0 \epsilon_w = (\pi/b)^2 - \kappa^2. \quad (2.2.7)$$

The field solution and separation equation for the region $0 \leq z \leq d$ are given by Equations 2.2.2 and 2.2.3, respectively.

Equating the electromagnetic field components as given by Equations 2.2.2 and 2.2.6 with $z = d$ yields two independent relationships. The ratio of these two results gives an expression for κ in terms of the physical parameters of the problem. Namely,

$$\kappa = -(\pi/c) \cot(\pi d/c). \quad (2.2.8)$$

For only one extremum of electric field intensity in the region $0 \leq z \leq d$ and under the constraint that $\kappa > 0$, the behavior of the cosecant function dictates that $c/2 < d < c$.

It is now possible to specify the ratio of ϵ_c to ϵ_w by eliminating $\omega_r^2 \mu_0 \epsilon_0 \epsilon_w$ between the separation Equations 2.2.3 and 2.2.7. The relation thus obtained is

$$\epsilon_c / \epsilon_w = (1 + (b/c)^2) / (1 - (b/c)^2 \cot^2(d/c)). \quad (2.2.9)$$

It may be noted that this equation is consistent with the inequality 2.2.5. Also, this equation may be rearranged to specify the dimension d in terms of the various other parameters.

The equation of the electromagnetic field terms for the two regions also determines the amplitude coefficient E_w . Making use of Equation 2.2.8 gives

$$E_w = \sin(\pi d/c) \exp((\pi d/c) \cot(\pi d/c)). \quad (2.2.10)$$

The electromagnetic field solution for the trapped mode resonator of Figure 2.2 is complete. The components of electric and magnetic field intensity are given by Equations 2.2.2 and 2.2.6 combined with Equations 2.2.8, 2.2.9, and 2.2.10. The solution is given in terms of the dimensions of the closed resonator with the desired resonant frequency.

The integrals involved in the calculation of the quality factor may now be formulated. It is convenient to delete the factor $1/j\omega\mu$ which is common to all of the magnetic field intensity terms. With such a deletion it may be shown that

$$\begin{aligned} \iiint_V |\underline{H}|^2 dv = & (ab/4) (d(1/c^2 + 1/b^2) \\ & + (c/\pi)(1/c^2 - 1/b^2) \sin(2\pi d/c) \\ & + (1/\kappa)(\cos^2(\pi d/c)/c^2 + \sin^2(\pi d/c)/b^2)) \end{aligned} \quad (2.2.11)$$

and

$$\begin{aligned} \iint_S |\underline{H}|^2 |ds| = & ab/2c^2 + (a/b^2) [d - (c/\pi) \sin(2\pi d/c) \\ & + (1/\kappa) \sin^2(\pi d/c)] + (b/2) [d(1/c^2 + 1/b^2) \\ & + (c/\pi)(1/c^2 - 1/b^2) \sin(2\pi d/c) \\ & + (1/\kappa)(\cos^2(\pi d/c)/c^2 + \sin^2(\pi d/c)/b^2)]. \end{aligned} \quad (2.2.12)$$

When the above two expressions are substituted into Equation 2.1.5, the resulting expression is one which is not easily compared with the

result for the closed resonator (Equation 2.2.4). In order to facilitate a comparison, a specific example will be considered.

Consider that the dimensions of the closed resonator are such that $2a = b = c$. With this choice, Equation 2.2.5 forces that the ratio of the relative dielectric constants be greater than 2. For this example, consider that $\epsilon_c = 2.25$ and $\epsilon_w = 1.0$. These values are typical of polystyrene and free space, respectively. Recall that there has been no loss within the dielectric itself considered.

Using Equation 2.2.9, the dimensions c and d may be related as

$$d/c = (1/\pi)\tan^{-1}(-3) = 0.60242. \quad (2.2.13)$$

(It has been shown that $c/2 < d < c$ must be satisfied and hence the choice of the minus sign on the argument of the inverse tangent function.)

Substitution of the dimensional constraints into Equation 2.2.4 yields for the closed resonator

$$Q_{011}^{\text{closed}} = (\omega\mu/R_s)(b/8). \quad (2.2.14)$$

For the trapped-mode resonator, Equations 2.1.5, 2.2.11, and 2.2.12 supplemented by Equations 2.2.8 and 2.2.13 give the result that

$$Q_{011}^{\text{open}} = (\omega\mu/R_s)(b/8)(1.656) \quad (2.2.15)$$

or

$$Q_{011}^{\text{open}}/Q_{011}^{\text{closed}} = 1.656. \quad (2.2.16)$$

Thus, the replacement of one conducting wall of a closed resonator (with the specific dimensional relationships considered) with a reactive surface formed by a section of cutoff waveguide, and the modification of the physical size of the dielectric in the previously closed resonator, results in an increased quality factor.

C. Cylindrical Geometry: Circulating Electric Field Mode

The example to be considered next was chosen because of its similarity to a somewhat frequently used trapped-mode configuration (20, 23-25, 27). The example is that of a cylindrical resonator with radius a and axial length d (both in meters; see Figure 2.3) which is operated in the TE_{011} mode (nomenclature is that of Harrington (13)). In this mode, the electric field may be thought of as circulating about the axis of the resonator. For this solid cylindrical wall configuration there is degeneracy with the TM_{111} mode. The analysis below assumes that this latter mode is not present.

For the coordinate system shown in Figure 2.3, an appropriate expression for the electromagnetic field within the resonator is

$$\begin{aligned}
 E_{\phi} &= \sin(\pi z/d) J_1(3.832r/a) \\
 H_r &= (\pi/j\omega\mu d) \cos(\pi z/d) J_1(3.832r/a) \\
 H_z &= (-3.832/j\omega\mu a) \sin(\pi z/d) J_0(3.832r/a) \\
 E_r &= E_z = H_{\phi} = 0.
 \end{aligned}
 \tag{2.3.1}$$

The separation equation is

$$\omega_r^2 \mu_0 \epsilon_0 \epsilon_c = (\pi/d)^2 + (3.832/a)^2.
 \tag{2.3.2}$$

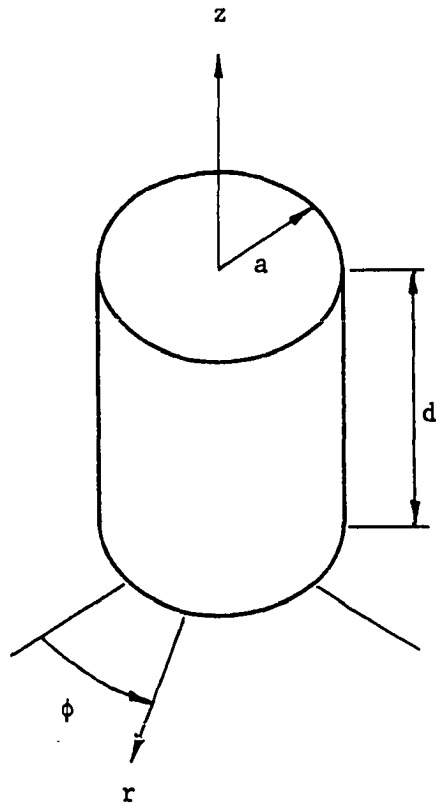


Figure 2.3. Closed cylindrical resonator

Evaluation of Equation 2.1.5, using the field given by Equation 2.3.1 gives the result:

$$Q_{011}^{\text{closed}} = \frac{\omega\mu da^2 (\pi/d)^2 + (3.832/a)^2}{R_s 2 2(\pi a/d)^2 + ad(3.832/a)^2} \quad (2.3.3)$$

The trapped-mode resonator to be considered is one similar to that above but with the cylindrical surface removed and a cutoff radial waveguide attached in its place to create a reactive surface. In order that the resonant frequency not be changed, the radius of the dielectric with permittivity ϵ_c must be changed to c meters. The trapped-mode resonator thus formed is shown in Figure 2.4.

The electromagnetic field solution for the region $r > c$ in Figure 2.4 is

$$\begin{aligned} E_\phi &= E_w \sin(\pi z/d) K_1(\kappa r) \\ H_r &= (E_w \pi / j \omega \mu d) \cos(\pi z/d) K_1(\kappa r) \\ H_z &= (E_w \kappa / j \omega \mu) \sin(\pi z/d) K_0(\kappa r) \\ E_r &= E_z = H_\phi = 0 \end{aligned} \quad (2.3.4)$$

where E_w is an amplitude coefficient which is to be determined. The separation equation is

$$\frac{\omega^2 \mu \epsilon_c \epsilon_w}{r^2} = (\pi/d)^2 - \kappa^2 \quad (2.3.5)$$

The requirement that the resonant frequency of the closed cavity be greater than the cutoff frequency of the radial waveguide gives that

$$\epsilon_c / \epsilon_w > 1 + (3.832d/\pi a)^2 \quad (2.3.6)$$

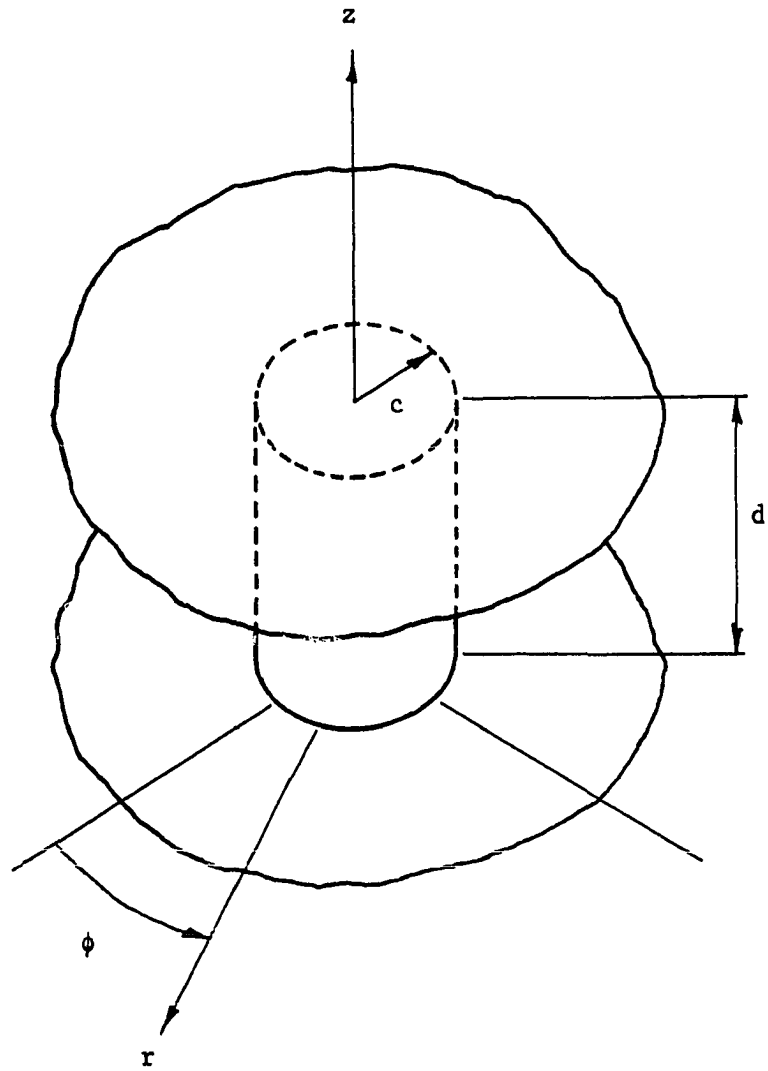


Figure 2.4. Trapped-mode cylindrical resonator

Further, eliminating $\omega_r^2 \mu_0 \epsilon_0$ between Equations 2.3.2 and 2.3.5 gives

$$\epsilon_c / \epsilon_w = (1 + (3.832d/\pi a)^2) / (1 - (\kappa d/\pi)^2) \quad (2.3.7)$$

which clearly satisfied the inequality 2.3.6. Alternatively, Equation 2.3.7 may be rearranged to be

$$\kappa^2 = (\pi/d)^2 (1 - \epsilon_w / \epsilon_c) - (\epsilon_w / \epsilon_c) (3.832/a)^2. \quad (2.3.8)$$

Equating field components at $r = c$ gives two independent relationships. Namely,

$$J_1(3.832c/a) = E_w K_1(\kappa c) \quad (2.3.9)$$

and

$$(-3.832/a) J_0(3.832c/a) = E_w \kappa K_0(\kappa c). \quad (2.3.10)$$

Dividing Equation 2.3.10 by Equation 2.3.9 gives

$$\frac{-3.832}{a} \frac{J_0(3.832c/a)}{J_1(3.832c/a)} = \kappa \frac{K_0(\kappa c)}{K_1(\kappa c)}. \quad (2.3.11)$$

Now, given the physical parameters a , d , ϵ_c , and ϵ_w , Equation 2.3.11 may be solved (with the aid of Equation 2.3.8) for the dimension c . This is not a direct process; however, a trial-and-error process on a digital computer is quite effective. When c is determined, E_w may be determined by use of Equation 2.3.9 and the electromagnetic field solution for the trapped-mode resonator is complete.

Finally, the quality factor is evaluated using the field solution and Equation 2.1.5. The result is

$$Q_{011}^{\text{open}} = (\omega\mu d/4R_s) \{1 + (kd/\pi)^2/[J_0^2(kc)/J_1^2(kc) - (2/kc)(J_0(kc)/J_1(kc))]\} \quad (2.3.12)$$

where $k = 3.832/a$.

As was true for the previous example, the resulting expression for the quality factor for the trapped-mode resonator is not easily compared to the corresponding result for the closed resonator. Therefore, a specific numerical result will be given. If the relationship $a = d$ is imposed, then Equation 2.3.6 requires that $\epsilon_c/\epsilon_w > 2.487$. If ϵ_c is chosen to be 3.0 and ϵ_w is chosen to be 1.0 then Equation 2.3.8 may be evaluated for the value of κ . A trial and error procedure using Equation 2.3.10 gives the result that $c/a = 0.68402$.

With these constraints,

$$Q_{011}^{\text{closed}} = (\omega\mu d/R_s)(0.35665) \quad (2.3.13)$$

and

$$Q_{011}^{\text{open}} = (\omega\mu d/R_s)(0.43814) \quad (2.3.14)$$

so that

$$Q_{011}^{\text{open}}/Q_{011}^{\text{closed}} = 1.228. \quad (2.3.15)$$

As was true in the previous example, the replacement of a conducting wall of a closed resonator with a reactive surface formed by a

cutoff waveguide has resulted in an increased quality factor. Further, although it has not been shown here, it should be noted that the degeneracy has also been removed by the modification in the cylindrical boundary.

III. ANALYSIS OF TRAPPED-MODE STRUCTURES: APPROXIMATE SOLUTIONS

A. Introductory Comments

The solutions examined in the previous section were characterized by the fact that an exact solution of the electromagnetic field problem for the lossless situation is possible. Some trapped-mode resonator configurations, however, are not so easily solved in that the electromagnetic field solution in the vicinity of the reactive surface is not known.

An example of such a configuration is that considered by Potter (25). His analysis considers the reactive surface to be a periodic structure and uses an analytical technique similar to that of Watkins (32). While Potter's results agree quite well with his analysis, extension of the analysis to structures possessing other than a simple periodicity is not direct.

A technique which may be utilized for resonant frequency studies is a variational formulation. Such a formulation is discussed by Harrington (13) and was used by Morton (23) for the analysis of a tunable trapped-mode resonator. This technique has the advantage that the parameter expressed by the variational formula has a stationary form: a form which is relatively insensitive to the accuracy of the choice of the approximate electromagnetic field solution. (The choice of an approximate solution is implicit in that an exact solution is not known.)

A variational formulation for a class of assumed trial fields is developed below. Since the complex angular resonant frequency is formulated, the losses (and hence the quality factor) may be inferred from the imaginary term (13).

The availability of a high-speed digital computer with large storage capacity makes practical the solution of partial differential equations by numerical methods (14, 15). Some considerations of a program are discussed below and a program to solve a specific example trapped-mode resonator is discussed in Appendix B and listed in Appendix C.

B. Variational Formulation

As discussed in the introduction, resonance is said to exist when the time-average electric and magnetic energies within the volume of the cavity are equal. This condition exists at certain frequencies; hence, it is desired to formulate an expression which will give the resonant frequency in terms of the electromagnetic field. Or, since the electric and magnetic field intensities may be related, the resonant frequency might be expressed as a function of either the electric or magnetic field intensity. Assume that the resonator is such that the formulation of the exact electromagnetic field solution is practically impossible. Thus, some sort of trial field will have to be estimated and it will be necessary to formulate the resonant frequency of the structure in terms of the trial field. Then, in order that the resonant frequency calculation be valid, it is desirable to have the resonant frequency equation in a stationary form.

Consider that the trial field is given by

$$\underline{E}_{\text{trial}} = \underline{E} + p\underline{e}, \quad (3.2.1)$$

where \underline{E} represents the exact (but unknown) solution and \underline{e} is the unscaled error in $\underline{E}_{\text{trial}}$, is used to formulate ω^2 , the square of the angular resonant frequency of a cavity. Then, the Maclaurin expansion of ω^2 as a function of p is

$$\begin{aligned} \omega^2(p) = \omega_r^2 + p \left[\frac{\partial \omega^2}{\partial p} \Big|_{p=0} \right] + \frac{p^2}{2!} \left[\frac{\partial^2 \omega^2}{\partial p^2} \Big|_{p=0} \right] \\ + \dots \end{aligned} \quad (3.2.2)$$

The first term of the expansion is ω_r^2 , the square of the true resonant frequency since $\omega^2(p=0) = \omega_r^2$.

In the variational notation (16) Equation 3.2.2 is written as

$$\omega^2(p) = \omega_r^2 + \delta\omega^2 + \delta^2\omega^2 + \dots \quad (3.2.3)$$

with a correspondence between the various terms of the two expansions.

A formula for ω^2 is said to be stationary if the first variation of ω^2 (i.e., $\delta\omega^2$) vanishes. This is equivalent to

$$\frac{\partial \omega^2}{\partial p} \Big|_{p=C} = 0. \quad (3.2.4)$$

Harrington (13) indicates that a complex ω^2 will have a saddle point at $p = 0$.

An important consideration is the procedure used to establish stationary formulas. One technique is to construct formulas to express

the desired parameter and then discard those which do not satisfy Equation 3.2.4. An alternative and more orderly procedure is to apply the reaction concept of Rumsey (28). The particular procedure as applied to the construction of stationary formulas is given by Harrington (13) and is the one used below. Berk (4) also discusses variational principles for resonator and waveguide problems.

The trapped-mode resonators to be considered are characterized by two physical sections. One section is not unlike a conventional closed resonator except that its boundary has been modified by the attachment of the other section. The second section is such that it presents a reactive surface at the point of attachment to the first section. Since the transition between the two sections is generally quite abrupt, an exact electromagnetic field solution is difficult if not impossible. It is this difficulty which the use of a variational formula will help to overcome.

The purpose now is to establish a stationary formula which will be appropriate to determine the resonant frequency of a trapped-mode resonator which is characterized as above. To that end, consider first the nature of the trial field which might be used.

Since one section of the trapped-mode resonator is similar to a closed resonator, assume that the lossless electromagnetic field solution corresponding to such a closed resonator is known. Such a resonator is depicted in Figure 3.1a. Over any surface s which is within or on the boundary of the resonator (shaded surface in Figure 3.1b) the tangential electric field $\underline{n} \times \underline{E}$ and a term related to the tangential

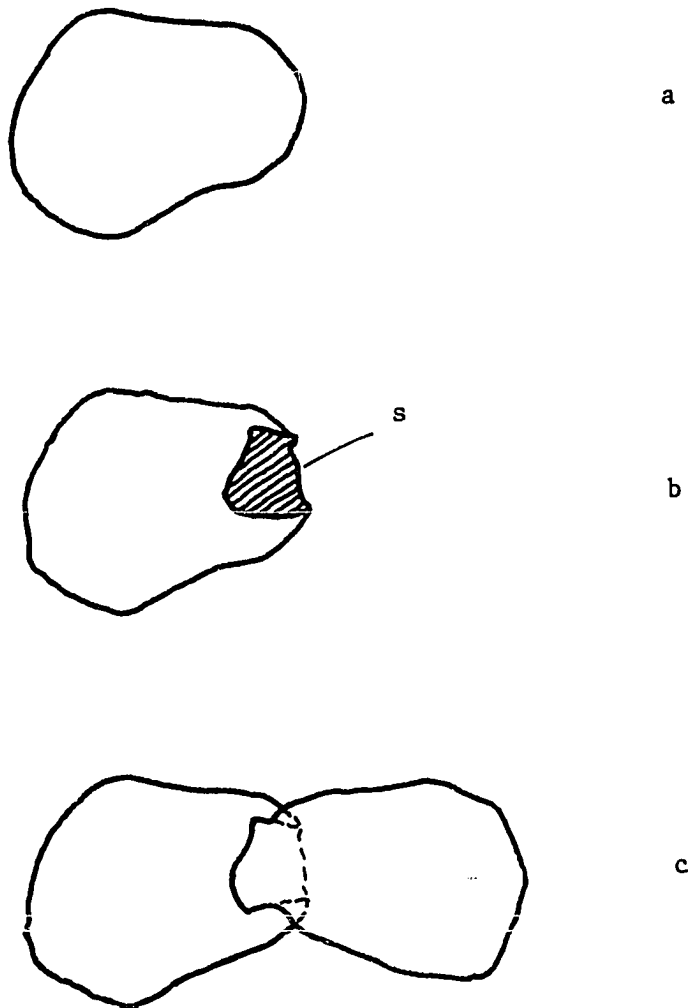


Figure 3.1. Symbolic trapped-mode resonator development

magnetic field $\underline{n} \times (\mu^{-1} \underline{\nabla} \times \underline{E})$ are known. If a reactive surface is established over s by the attachment of a second section as depicted in Figure 3.1c, then it is possible to formulate a trial field which will force continuity of either $\underline{n} \times \underline{E}$ or $\underline{n} \times (\mu^{-1} \underline{\nabla} \times \underline{E})$ (or possibly both) over s by means of an appropriate modal expansion in the newly attached section. This continuity of tangential electric or magnetic field intensity forces interdependence of the trial field in the two regions.

If the condition that $\underline{n} \times \underline{E}$ be continuous over s is chosen and if s coincides with the boundary of the original resonator of Figure 3.1a, then the (mathematical) coupling between the two regions vanishes since for the lossless solution the tangential electric field will now be zero on s . Hence, the choice of continuity of $\underline{n} \times (\mu^{-1} \underline{\nabla} \times \underline{E})$ over s is made to relate the trial field at the boundary of the two sections. Any resulting discontinuity of tangential electric field there will be accounted for in the development of the variational formula below.

Rumsey (28) defines the reaction of the electromagnetic field resulting from a source distribution a upon the source distribution b as

$$\langle a, b \rangle = \iiint_V (\underline{E}_a \cdot d\underline{J}_b - \underline{H}_a \cdot d\underline{M}_b) \quad (3.2.5)$$

where $\exp(j\omega t)$ time-dependence is implicit. He further interprets that if all media are isotropic and the sources a and b are both within V , then reciprocity gives that

$$\langle a, b \rangle = \langle b, a \rangle. \quad (3.2.6)$$

Harrington (13) establishes that since for a resonator the true field at resonance is a source-free field the reaction of any field with the true source is zero or, more specifically,

$$\langle a, a \rangle = 0. \quad (3.2.7)$$

It is necessary to insure that the formula for the desired parameter (which is to be determined from the reaction) is stationary. Here, the concern is with the (angular) resonant frequency ω . Considering equation 3.2.7 as both ω and p are varied (about ω_r and zero, respectively) we get that

$$\left[\frac{\partial \langle a, a \rangle}{\partial \omega} \right]_{\substack{\omega = \omega_r \\ p = 0^r}} \delta \omega + \left[\frac{\partial \langle a, a \rangle}{\partial p} \right]_{\substack{\omega = \omega_r \\ p = 0^r}} \delta p = 0. \quad (3.2.8)$$

The coefficient of δp is zero since $\langle a, a \rangle$ is stationary about $p = 0$. Since the coefficient of $\delta \omega$ is not in general zero, it must be true that $\delta \omega = 0$. The first variation of the resonant frequency about $\omega = \omega_r$ and $p = 0$ as constrained by Equation 3.2.7 is zero.

Following with the development of Harrington (13), the application of Equation 3.2.7 is to assume a trial field which satisfies the convenient physical constraints and to determine its sources as follows: An assumed electric field may be supported by the electric current density given by

$$\underline{J} = -j\omega\epsilon\underline{E} - (1/j\omega)\underline{\nabla} \times (\mu^{-1}\underline{\nabla} \times \underline{E}). \quad (3.2.9)$$

If the trial field violates the condition that $\underline{n} \times \underline{E} = 0$ on any surface (including the resonator boundary) then the source

$$\underline{M}_s = \underline{n} \times \underline{E} \quad (3.2.10)$$

must be added at that surface to support the discontinuity. Now, Equations 3.2.5, 3.2.7, 3.2.9, and 3.2.10 may be combined to give a stationary formula in terms of an assumed electric field intensity \underline{E} .

In a similar manner, a stationary formula in terms of an assumed \underline{H} may be developed as may a so-called hybrid formula in terms of assumed \underline{E} and \underline{H} . The details of these developments are given in Harrington (13) and will not be repeated here.

The formulation of the losses is based upon the small-loss approximation discussed in the introductory comments of the previous section of this thesis. Further discussion of this approximation is available in various references (5, 13, 26).

The restrictions placed upon the stationary formula to be generated are as follows:

- 1) The formula will be in terms of a trial electric field intensity \underline{E} which satisfies $\underline{n} \times \underline{E} = 0$ on the conducting boundary surfaces;
- 2) Discontinuity of $\underline{n} \times \underline{E}$ over boundary or internal partitioning surfaces will be accounted for;
- 3) Continuity of tangential magnetic field intensity (that is, continuity of $\underline{n} \times (\mu^{-1} \underline{\nabla} \times \underline{E})$) will be required everywhere except at conducting surfaces where the discontinuity will be supported by an appropriate electric surface current density.

Two situations for discontinuity of $\underline{n} \times \underline{E}$ present themselves: at the junction of the two sections of the resonator volume and at good (but imperfectly) conducting boundaries. The development below characterizes the surfaces over which these discontinuities exist according to the schematic representation of the resonator as depicted in Figure 3.2.

The surface s in Figure 3.2 is intended to represent the surface or surfaces within the volume of the resonator over which discontinuity in $\underline{n} \times \underline{E}$ is to be considered. This discontinuity is supported by the magnetic surface current

$$\underline{M}_s = \underline{n} \times (\underline{E}_2 - \underline{E}_1). \quad (3.2.11)$$

The surface S in Figure 3.2 is intended to represent the conducting boundary of the resonator. The discontinuity there is due to the imprecise nature of the trial field and is due therefore, to the lack of continuity of the chosen mathematical expression with physical reality. For a good conductor, the surface impedance (13) is given by $Z_s = R_s(1 + j)$. The electric surface current density induced in the conducting walls is equal in magnitude but normal to the tangential magnetic field intensity there. In terms of the assumed trial field,

$$\underline{J}_s = -(1/j\omega_r)\underline{n} \times (\mu^{-1}\underline{\nabla} \times \underline{E}) \quad (3.2.12)$$

where the surface current density \underline{J}_s is consistent with the lossless trial field. Its value is such that the total electric current flowing per unit width is the same for the assumed lossless and the non-loss-free

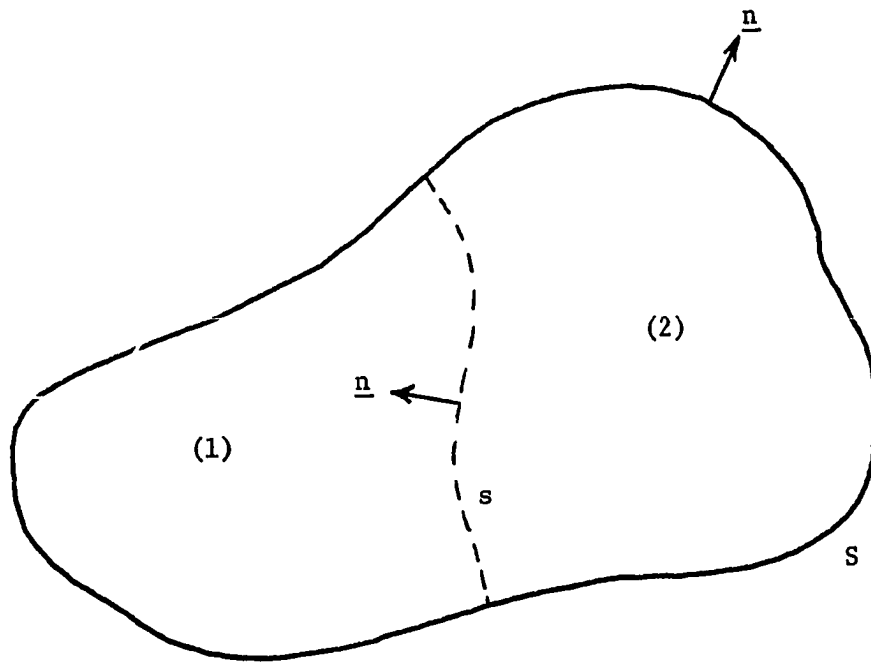


Figure 3.2. Generalized trapped-mode resonator

situations. Thus the (perturbing) electric field at S must be

$$\underline{E} = Z_s \cdot \underline{J}_s \text{ or,}$$

$$\underline{E} = - (R_s (1 + j) / j\omega_r) \underline{n} \times (\mu^{-1} \underline{\nabla} \times \underline{E}). \quad (3.2.13)$$

The magnetic surface current density necessary on S to support this electric field intensity is given by $-\underline{n} \times \underline{E}$ or,

$$\underline{M}_s = (R_s (1 + j) / j\omega_r) [(\underline{n} \cdot (\mu^{-1} \underline{\nabla} \times \underline{E}))^2 - (\mu^{-1} \underline{\nabla} \times \underline{E})^2] \quad (3.2.14)$$

after a standard vector identity has been applied.

With the expression of magnetic field intensity in terms of the trial field as

$$\underline{H} = (1/j\omega) (\mu^{-1} \underline{\nabla} \times \underline{E}), \quad (3.2.15)$$

the reaction given by Equations 3.2.7 and 3.2.5 may be formulated. The result is

$$0 = \iiint_V [-j\omega\epsilon \underline{E}^2 - (1/j\omega) \underline{E} \cdot \underline{\nabla} \times (\mu^{-1} \underline{\nabla} \times \underline{E}) - (1/j\omega) \underline{M}_s \cdot (\mu^{-1} \underline{\nabla} \times \underline{E}) - (1/j\omega) \underline{M}_s \cdot (\mu^{-1} \underline{\nabla} \times \underline{E})] dv. \quad (3.2.16)$$

Of the four integrals implied above, the last three may be put into simpler form after the simplifying operation of multiplication by ω/j .

The second term may be rearranged as follows: Recall the vector identity $\underline{\nabla} \cdot (\underline{A} \times \underline{B}) = \underline{B} \cdot (\underline{\nabla} \times \underline{A}) - \underline{A} \cdot (\underline{\nabla} \times \underline{B})$. Making the identifications $\underline{A} = \underline{E}$ and $\underline{B} = \mu^{-1} \underline{\nabla} \times \underline{E}$, the integrand becomes $\mu^{-1} (\underline{\nabla} \times \underline{E})^2 - \underline{\nabla} \cdot (\underline{E} \times (\mu^{-1} \underline{\nabla} \times \underline{E}))$. The second term in this integrand is now the

divergence of a vector field and so may be treated using the divergence theorem. Then, noting that $\underline{E} \times (\mu^{-1} \underline{\nabla} \times \underline{E}) \cdot d\underline{s} = (\mu^{-1} \underline{\nabla} \times \underline{E}) \cdot (d\underline{s} \times \underline{E}) = 0$ on S since the tangential component of the trial field vanishes on S , this latter term vanishes.

The third term has value only on the interior surface s . Thus the volume over which the integration is performed may be allowed to collapse until only s is enclosed. Then, there is an equal contribution on each side of s so that the third integral becomes $2 \iint_s \underline{n} \times (\underline{E}_2 - \underline{E}_1) \cdot (\mu^{-1} \underline{\nabla} \times \underline{E}) |d\underline{s}|$. Using the scalar triple product, this becomes $2 \iint_s (\underline{E}_2 - \underline{E}_1) \times (\mu^{-1} \underline{\nabla} \times \underline{E}) \cdot d\underline{s}$.

The final term in integrand of Equation 3.2.16 is zero everywhere except on the boundary surface of the resonator. Therefore a surface integration is appropriate for that term.

Finally, solving for ω^2 gives the desired form. Namely,

$$\omega^2 = \frac{1}{\iint_V \epsilon \underline{E}^2 dv} \left[\iint_V \mu^{-1} (\underline{\nabla} \times \underline{E})^2 dv + 2 \iint_s (\underline{E}_1 - \underline{E}_2) \times (\mu^{-1} \underline{\nabla} \times \underline{E}) \cdot d\underline{s} - \frac{R_s (1+j)}{\omega_r} \iint_S (\underline{M} \times \mu^{-1} (\underline{\nabla} \times \underline{E}))^2 |d\underline{s}| \right] \quad (3.2.17)$$

It should be noted that even though this formula was developed with application to a trapped-mode resonator in mind, it may be applied to any problem for which the trial field meets the constraints listed on page 32.

C. Finite-difference Formulation

The availability of digital computers with large storage capability and high calculation speed has made practical the solution of partial differential equations by techniques which are impractical by hand calculation. Harrington addresses himself to the formulation of a variety of field problems for solution on a digital computer in References 14 and 15. Davies and Muilwyk (8) discuss considerations of solving the problem of the waveguide with uniform cross section with a digital computer program which uses finite-difference techniques. Beaubien and Wexler give attention to extending the work of Davies and Muilwyk to higher order modes (2) and to the calculation of attenuation coefficients of these higher order modes (3). A nearly universal reference on the subject of finite-difference methods for partial differential equations is that by Forsythe and Wasow (10).

The problem of interest is that of solving the Helmholtz equation

$$(\nabla^2 + \lambda)\phi = 0, \lambda > 0 \quad (3.3.1)$$

subject to appropriate boundary conditions on ϕ . Generally, ϕ is taken to be a scalar which represents one component of a vector potential field which is pertinent to the specific problem being considered. (The approach used for the example in this thesis, however, is slightly different from those cited above (2, 3, 8, 14, 15) in that the problem considered is not that of finding the electromagnetic field in a waveguide of uniform cross section but that of finding the field in a resonator configuration where only one component of electric field

intensity is known to exist. Thus the partial differential considered in the example discussed in Appendix B is not quite that given by Equation 3.3.1. This difference does not affect the application of this discussion.)

The function ϕ (indeed, an eigenfunction) is represented at discrete mesh points within the boundary of interest. Since many waveguide problems (those with uniform cross section) have known dependence upon one special coordinate, the problem considered is usually that of Equation 3.3.1 with the Laplacian operator replaced by the transverse Laplacian operator. Discretization converts the continuous problem to the matrix eigenvalue problem given by

$$(A - \lambda I)\phi_d = 0 \quad (3.3.2)$$

where the subscript d is used to emphasize that the problem is now a discrete one.

If the number of points in the mesh is not too large, the matrix eigenvalue problem of Equation 3.3.2 may be solved by hand by conventional techniques (9). Large matrices may be inverted by means of digital computer routines. The accuracy of this latter technique may depend somewhat upon the care used in formulation of the problem in that the cumulative round-off error may be significant compared to the elements of the resulting matrix (15). However, solution in this manner does have the advantage that all of the eigenvalues of the discrete problem are determined.

An alternative approach to the solution of Equation 3.3.2 is the use of a relaxation technique which calculates, iteratively, each

element of the array of points representing ϕ in terms of the values at the adjacent points, using a guessed eigenvalue. (The construction of an appropriate relationship for such a calculation is described in Appendix B.) After several (a few) iterations over the array, an estimate of the eigenvalue is made by using a discrete form of the Rayleigh quotient

$$\lambda = -\iint \phi \nabla^2 \phi \, ds / \iint \phi^2 \, ds. \quad (3.3.3)$$

Then, since the relaxation technique depends upon the eigenvalue λ , the array representing ϕ is recalculated and new estimates for λ made until the eigenvalue is determined. The convergence of this procedure is enhanced by the use of a so-called over-relaxation technique such as that described in Reference 8.

Generally, the eigenvalue will converge somewhat faster than will the array representing ϕ in that the Rayleigh quotient is a stationary form. Therefore, if accurate determination of ϕ_d is desired, the relaxation process should be continued somewhat beyond the time when the convergence of the eigenvalue is ascertained.

A specific example employing the technique of finite differences is discussed in Appendix B. The purpose of that example is to solve a specific trapped-mode resonator and to calculate the corresponding quality factor. The results of that example are given elsewhere in this thesis.

IV. EXPERIMENTAL INVESTIGATION

A. Experimental Resonator Design

In an effort to physically realize a simple trapped-mode resonator design which could be used to provide data to compare with analytical results, the design described below was chosen.

A closed resonator with cylindrical geometry was constructed as shown in an exploded view in Figure 4.1 from a stack of seven brass plates which were approximately four inches square. The five internal plates each had a thickness of 0.1882 inches and had a hole in their center with a diameter of 1.9190 inches. The end plates were solid except as described below. The assembly is held together by four screws, one at each corner of the plates.

Provision for coupling energy into the resonator was provided by means of two holes in one end plate. These two holes aligned with two similar holes in the sidewall of a piece of rectangular waveguide. The spacing between the centers of the two holes was approximately one-half of a guide wavelength at the frequencies of interest. An adjustable position shorting plane was placed in the waveguide just past the holes in order that the electric field pattern (a standing wave) in the guide could be adjusted so that relative maxima would be opposite the coupling holes. Since the holes are one-half wavelength apart, the field there will be of similar magnitude but out of phase by 180 degrees. Thus, there will be a tendency to excite the desired TE_{011} mode and to reject the unwanted TM_{111} mode. Recall that the two modes are degenerate in the solid wall configuration.

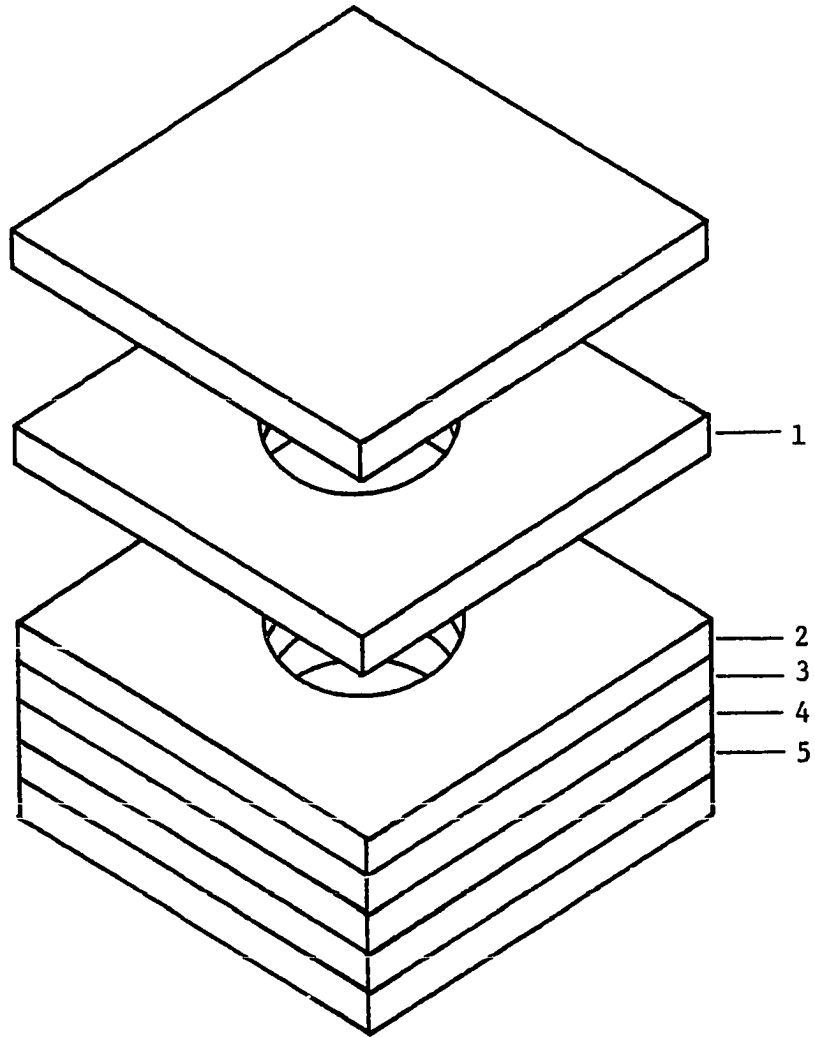


Figure 4.1. Experimental trapped-mode resonator (exploded view)

A trapped-mode structure was formed by replacing internal plates in the stack with spacers located at the corners. The spacers are made from material of the same thickness as the internal plates. In this way the axial length was kept constant. Three configurations were considered in the measurement program. Referring to Figure 4.1, one configuration was with plates numbered 1 and 5 replaced with spacers (called the semi-open configuration). The second configuration was with plates numbered 1, 2, 4, and 5 replaced with spacers (full-open configuration). The third configuration was that of the closed resonator (closed configuration). Figure 4.2 shows the assembled resonator in the semi-open configuration with the coupling structure attached.

It is important to insure that the radial dimension of the cutoff waveguide sections is great enough that there will not be significant field strength at the outer extremity of the plates. To that end, consider for the moment that instead of being square, the plates are circular with a radius $b = 2a$ where a is the radius of the hole in the plates. The axial length of the resonator will be denoted d and the thickness of the radial waveguide sections as t . (This notation is consistent with that used in Appendix A.)

Following the variational formulation developed in Appendix A, the electric field intensity in the cutoff radial section near $z = d$ is given by

$$E_{\phi}(r=b) = (1/(a\sqrt{\pi})) \sum_{n=1}^{\infty} k_n \sin(n\pi(z-d+t)/t) K_1(\kappa_n b)/K_1(\kappa_n a). \quad (4.1.1)$$

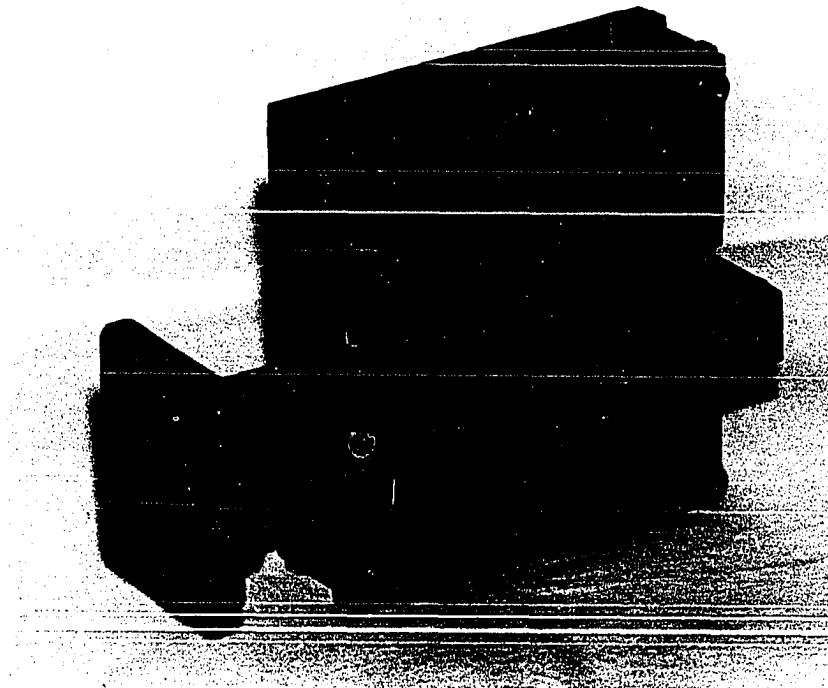


Figure 4.2. Assembled experimental trapped-mode resonator (semi-open configuration) with coupling structure attached.

The electric field intensity in the other cutoff radial section is similar to that given by Equation 4.1.1 except for changes of algebraic signs for some values of n . These expressions assume that there is no reflection of energy at $r = b$ or that all of the electric field at $r = b$ contributes to radiation of energy away from the resonator.

The power density at $r = b$ is given by $|E|^2/\eta$ where η is the intrinsic impedance of free space and is equal to $(\mu_0/\epsilon_0)^{1/2}$. Integrating this quantity over the surfaces where the electric field exists gives the power radiated from the n th order cutoff radial waveguide mode. With the use of the equation for k_n from Appendix A, the result is

$$P_{rn} = \frac{16(3.832)^2 t}{\eta \pi^2 a^3 \kappa_n^2} \frac{n^2}{(n^2 - (t/d)^2)^2} \sin^2(\pi t/d) (K_1(2\kappa_n a)/K_0(\kappa_n a))^2 \quad (4.1.2)$$

where κ_n is given by Equation A.3.

Calculation of the energy stored in the resonator by the techniques of Appendix A shows that essentially all of the energy is in the cylindrical volume and almost none in the cutoff radial sections. With a normalization which is consistent with Equation 4.1.1, the energy stored in the cylindrical volume may be shown to be

$$W = 2\bar{W}_e = d. \quad (4.1.3)$$

Finally, on the basis that the radiative loss is the only loss in the resonator, the quality factor may be formulated by the use of Equations 4.1.2 and 4.1.3 in Equation 2.1.1. The results for the first three ordered modes for the dimension t equal to $0.2d$ and $0.4d$ (corresponding to the semi- and full-open configurations, respectively, are

listed in Table 4.1. In all instances the quality factors listed are much larger than those due to the conductor losses so that radiation will be expected to produce negligible affect upon the measurements.

Table 4.1. Quality factors due to radiative effects

T/d	M	Q due to radiation
0.2	1	1.1×10^{25}
0.2	2	7.1×10^{39}
0.2	3	2.3×10^{54}
0.4	1	4.1×10^{16}
0.4	2	2.2×10^{24}
0.4	3	8.3×10^{31}

B. Measurement Technique

A laboratory set-up which is appropriate for the measurement of the quality factor of the various resonator configurations is shown schematically in Figure 4.3. The operation of the equipment is such that signals of similar magnitude and phase are applied to the reference and unknown loads. The signals reflected from the loads are sensed and compared by means of the microwave network analyzer--a device which may be used to determine the complex ratio of two high frequency signals. This apparatus comprises a reflectometer.

When operated as a measuring instrument the unknown load is the resonator under test and the reference load is a short circuit. The quantity displayed by the network analyzer in this situation is the

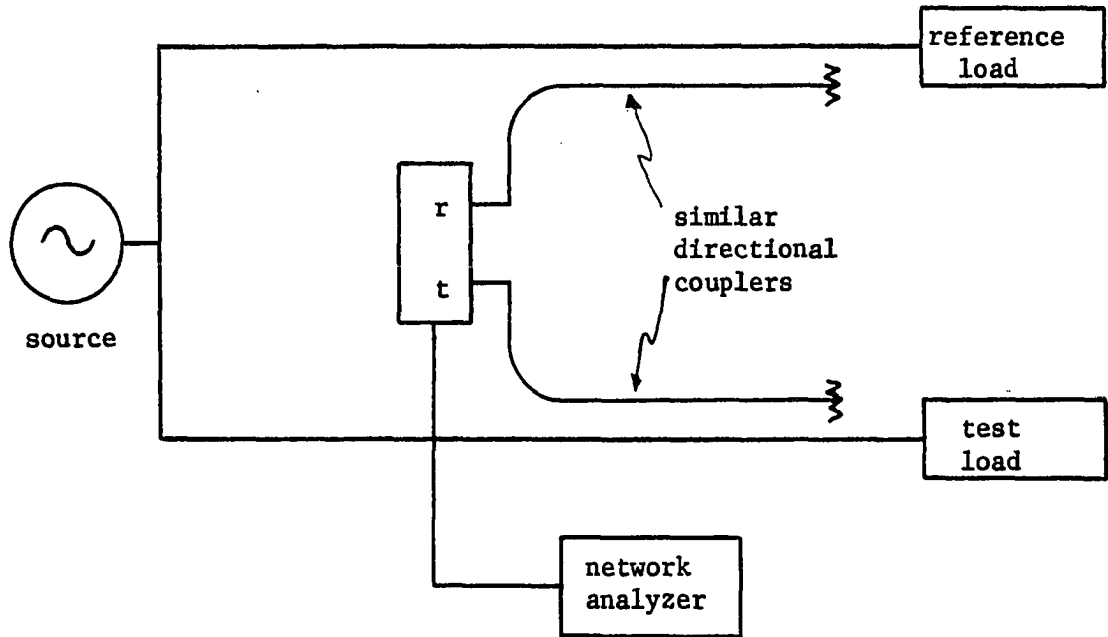


Figure 4.3. Basic experimental arrangement

reflection coefficient. In order to facilitate calibration of the measurement apparatus, the short circuit is a movable one in order that its position may be adjusted to correspond to the input port of the resonator in the measurement branch. Adjustment of this short circuit may be achieved by temporarily detuning the resonator under test and then positioning the short circuit so that equal signals are returned by both the test and measurement channels of the network analyzer.

Further, since the measurements are to be taken over a range of frequencies around the resonant frequency for each configuration of the resonator, and since the propagation of electromagnetic energy in waveguides is inherently dispersive, the reference and test channels must be physically symmetric if the measurements are to be correct at more than one frequency.

The particular equipment arrangement actually used is shown schematically in Figure 4.4. While this arrangement is operationally the same as is the arrangement shown in Figure 4.3, details of a practical laboratory set-up are included. Figure 4.5 shows the equipment as it appeared in the laboratory.

Since the particular coupling structure used provided very light coupling to the resonator under test, the phase of the reflection coefficient changed very little as the frequency of the signal which was applied to the cavity passes through resonance. Therefore, the data collected was on the basis of changes in the magnitude of the reflection coefficient around resonance. Ginzton (12) discusses considerations of quality factor data treatment at length and his comments are the basis of the experimental procedure used.

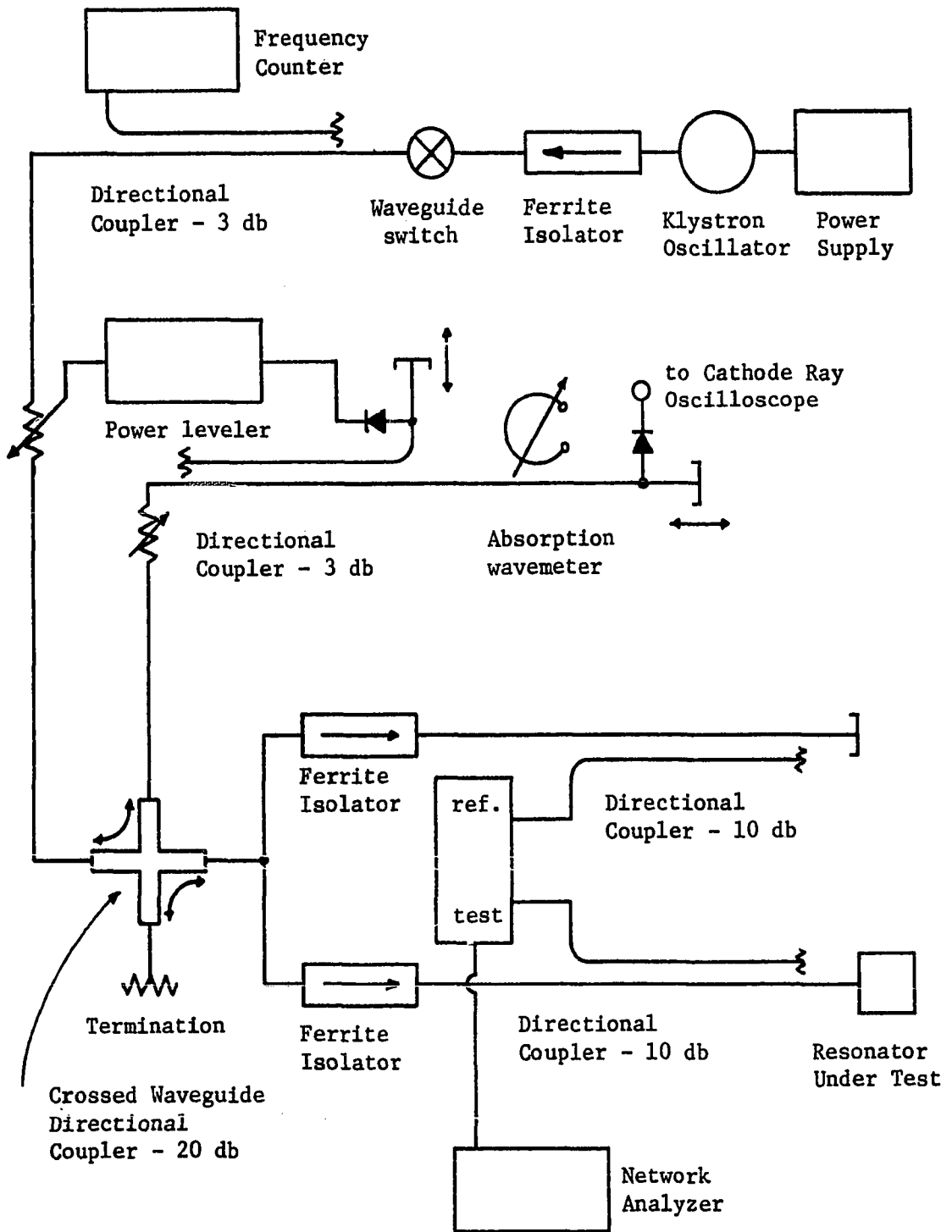


Figure 4.4. Detailed experimental arrangement

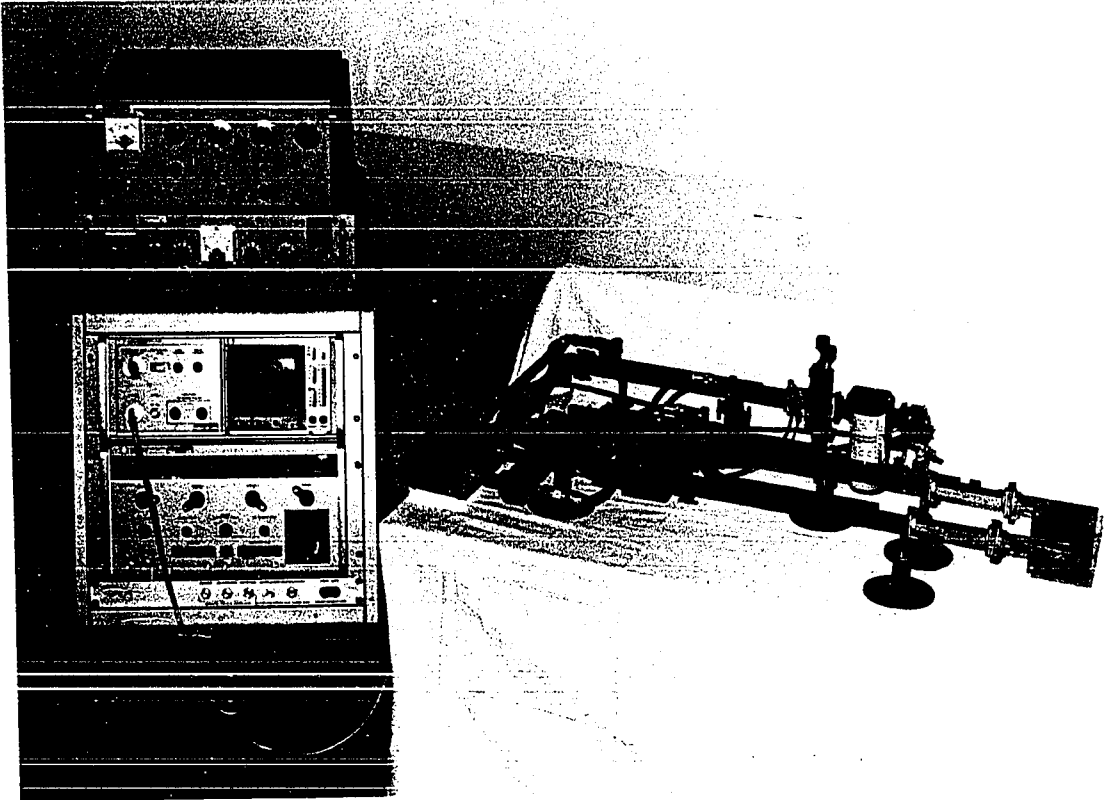


Figure 4.5. Actual laboratory arrangement. The frequency counter used for the measurements is not shown.

V. COMPARISON OF THEORETICAL AND EXPERIMENTAL DATA

In the preceding sections, analytical and experimental techniques which may be applied to trapped-mode resonators have been described. In order to provide comparison of experimental and the various analytical results for the various example resonator configurations which do not permit solution in closed form, corresponding physical dimensions were considered. (The details of the analyses of the specific example resonator are described in Appendices A and B.)

Figures 5.1 and 5.2 shows the resonant frequency data and Figures 5.3 and 5.4 show the corresponding quality factor data for the finite-difference and variational analyses and that from the corresponding laboratory measurements. For both figures, the abscissa is the thickness of one (of the two) radial waveguides divided by the axial length of the resonator. The data is given in tabular form in Table 5.1. The finite-difference analysis program used a discretization which divided axial and radial dimensions into thirty segments.

The vertical displacement of the experimental resonant frequency data from the analytical results is probably due to erroneous determination of the physical dimensions of the resonator. (Both analytical techniques give essentially the same result for the closed resonator). The finite difference result for the resonant frequency of the trapped-mode resonator corresponds quite well with the experimental data. The variation formulation result predict a somewhat larger frequency deviation as a result of opening the cavity than is observed.

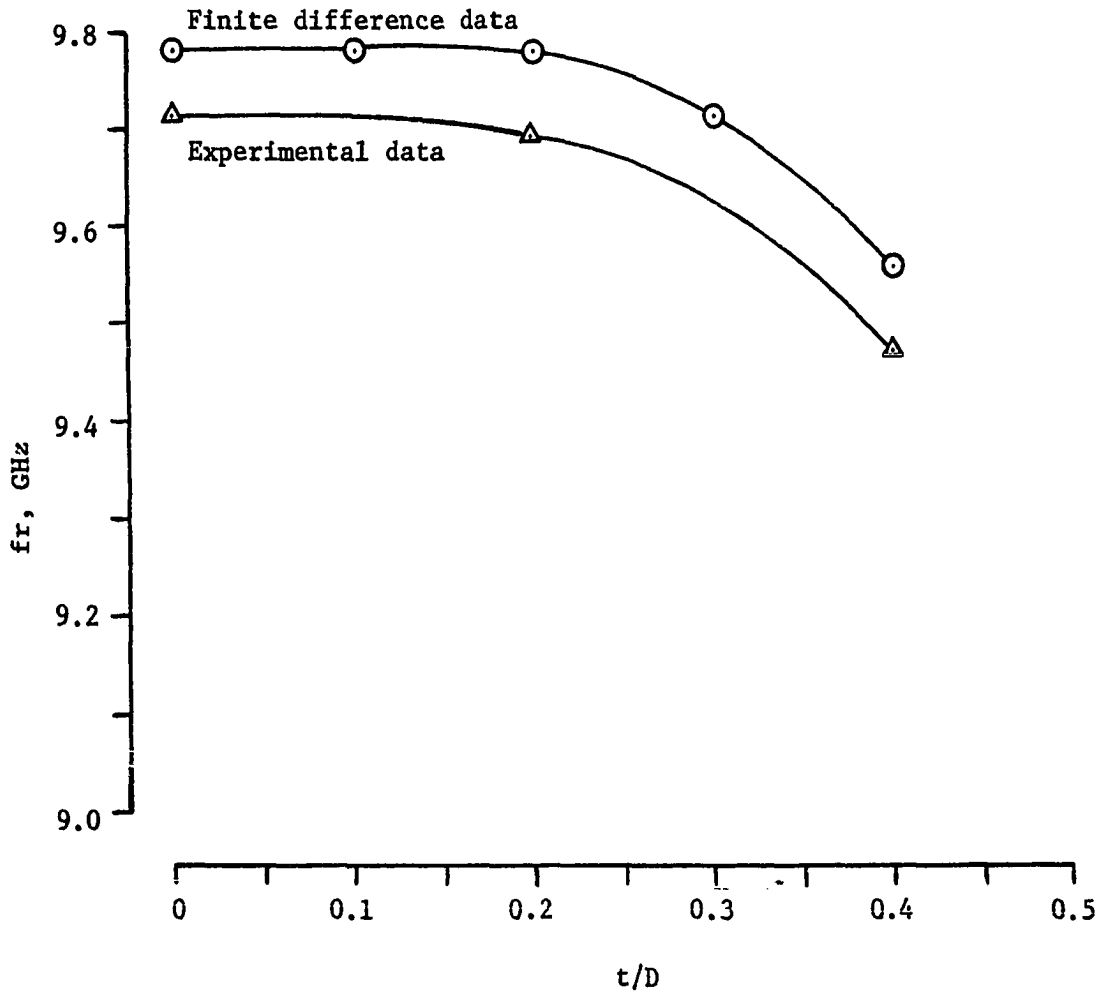


Figure 5.1. Resonant frequency vs. radial waveguide spacing: finite-difference and experimental data

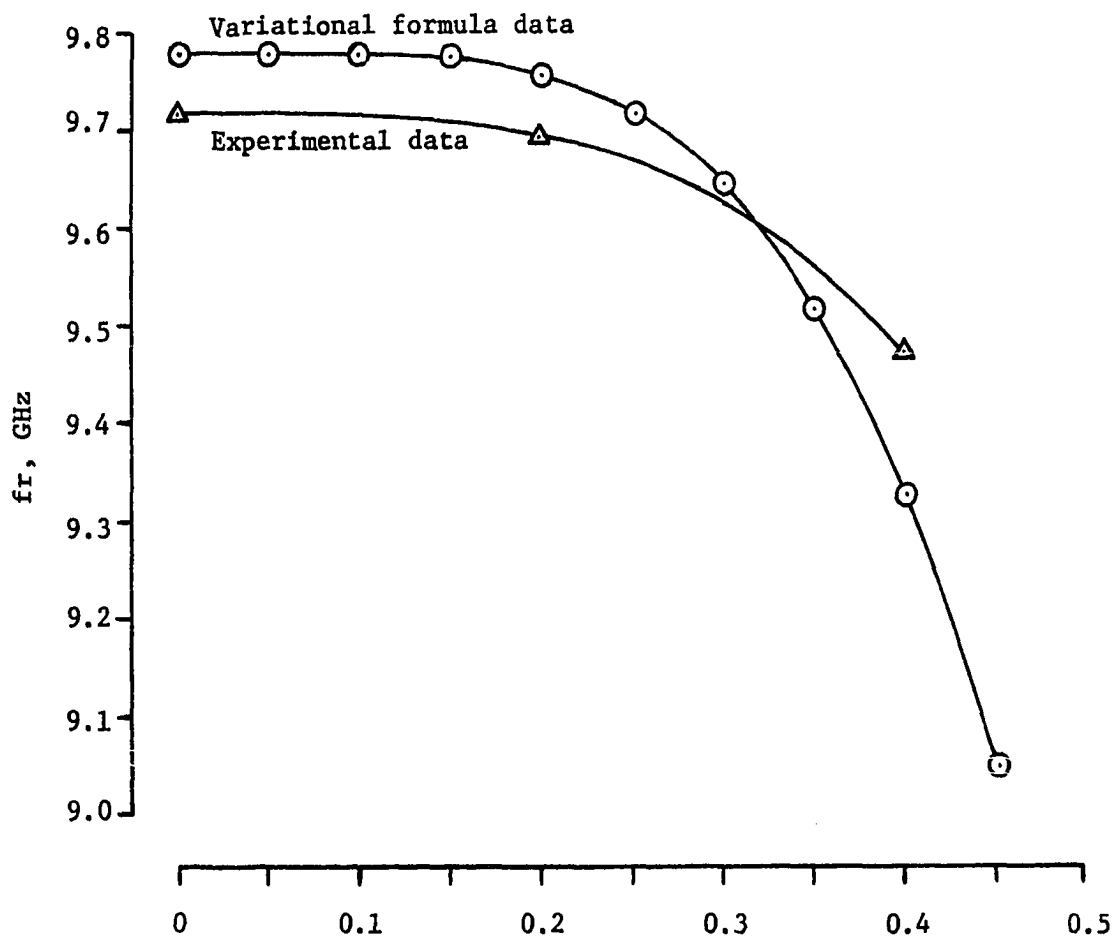


Figure 5.2. Resonant frequency vs. radial waveguide spacing: variational formulation and experimental data

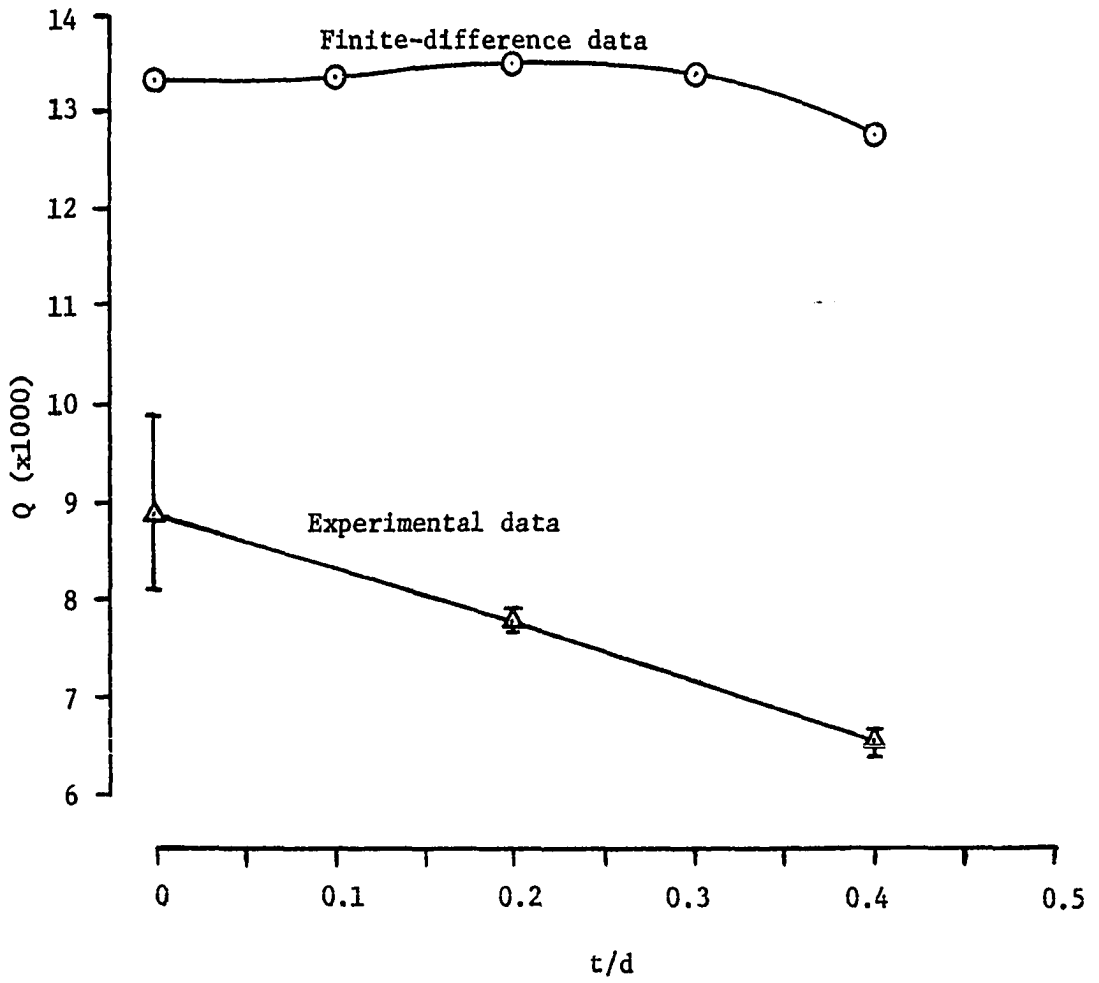


Figure 5.3. Quality factor data: finite-difference and experimental data

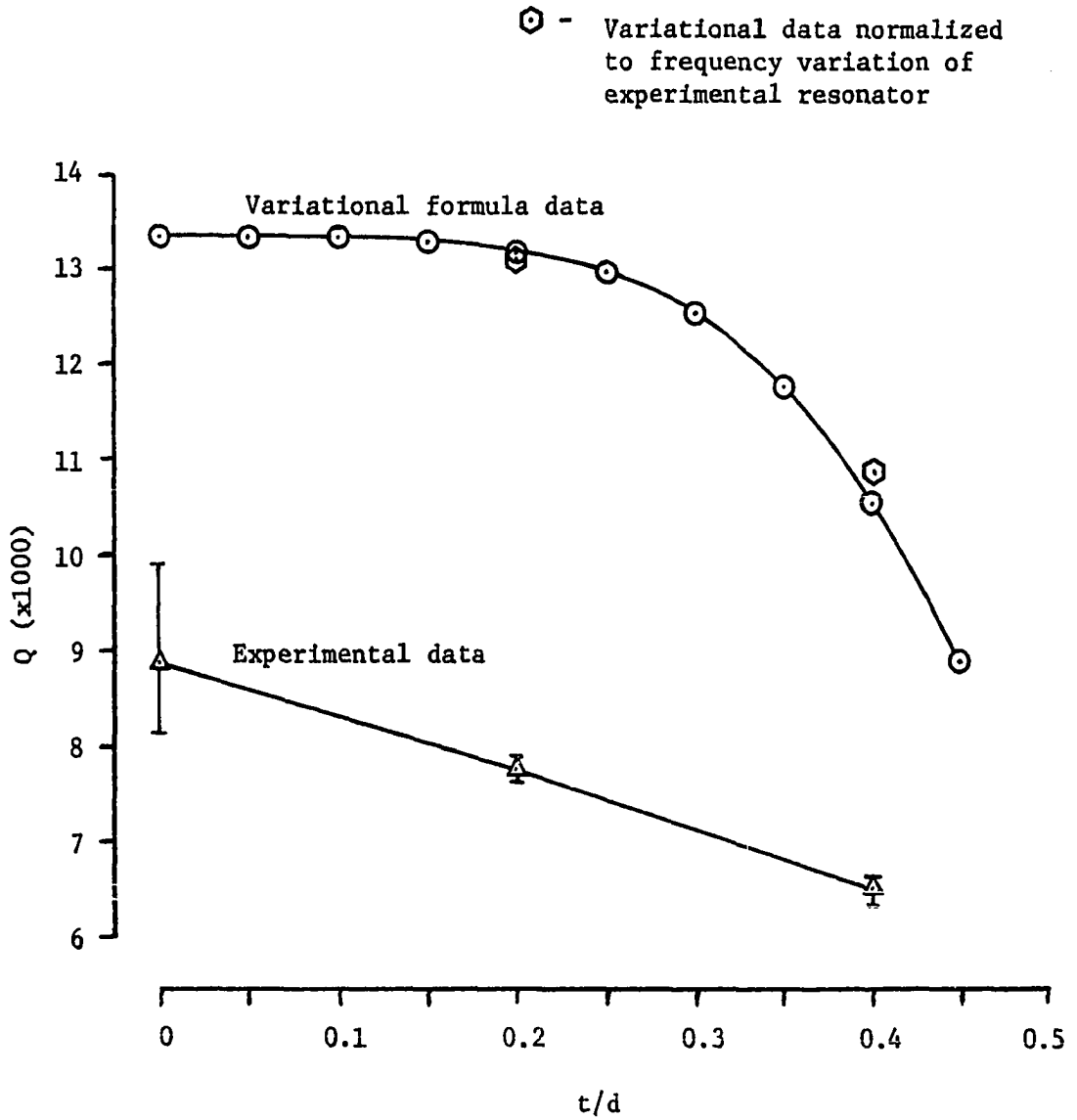


Figure 5.4. Quality factor data: variational formulation and experimental data

Table 5.1. Analytical and experimental results

t/d	Variational formulation		Finite- difference		Experimental	
	fr,GHz	Q	fr,GHz	Q	fr,GHz	Q
0	9.785	13307	9.781	13306	9.717	8860
0.05	9.784	13306	---	---	---	---
0.10	9.782	13301	9.780	13372	---	---
0.15	9.775	13271	---	---	---	---
0.20	9.756	13179	9.767	13470	9.690	7770
0.25	9.716	12962	---	---	---	---
0.30	9.642	12529	9.708	13380	---	---
0.35	9.518	11762	---	---	---	---
0.40	9.326	10551	9.550	12751	9.474	6530
0.45	9.047	8846	---	---	---	---

As is not unusual (21), the experimentally determined quality factor data is somewhat lower than is predicted. The cause of this discrepancy may lie among several possible items including incorrect wall material surface resistance characterization, lack of consideration of surface roughness or porosity (18), and unavoidable uncertainty in the measurement procedure.

One explanation which might account for the drop of experimental Q (as compared to the finite-difference result) might be that the radial cutoff waveguide sections in the experimental resonator were

not long enough to effect a complete reflection of the energy which entered them, thereby permitting some radiation from the resonator for the open configurations. For this to be true, however, the approximate calculations in the previous section would have to be greatly in error.

Figure 5.4 also shows two data points which correspond to a modification of the accompanying variational formulation data. The Q data is modified by using the resonant frequency data from the finite difference analysis. The result tends to indicate an increase in quality factor for larger values of t/d .

VI. SUMMARY AND CONCLUSION

Various aspects of the solution of trapped-mode resonators in both closed-form and approximate lossless formulations have been discussed and perturbation calculations for small wall-losses given.

Examples of rectangular and cylindrical closed resonators were compared to trapped-mode counterparts which were formed from the closed resonators by replacing part of the conducting boundaries with waveguides operating below cutoff. Conductor losses were compared for the closed and trapped-mode configurations at the same resonant frequency. The quality factor for the trapped-mode structure was found to be higher than that for the corresponding closed resonator for both of the geometries. Thus, the possibility of trapped-mode resonators with lower conductor losses than similar solid-wall resonators was established.

For those trapped-mode configurations which do not admit to exact lossless electromagnetic field solution, two approximate techniques were investigated. The first of these techniques was the establishment of a stationary variational formula for the square of the complex angular resonant frequency. The derivation used the reaction concept and was in terms of a trial electric field intensity which meets lossless boundary conditions at conducting surfaces. The possibility of discontinuity in the tangential electric field intensity within the resonator and upon the resonator boundary was included to permit easier formulation of a trial field. Effects of small conductor losses at resonator boundaries were also included.

The second approximate solution technique was that of a finite-difference formulation of the lossless electromagnetic field problem and the calculation of the corresponding small conductor losses. Details of the actual finite-difference problem formulation were considered and, in an Appendix, construction of a specific digital computer program was given.

The analysis of a specific trapped-mode resonator example was executed using the two approximate techniques which were investigated and the results compared with laboratory data for a similar resonator. In that comparison, the correlation of resonant frequency data for the finite-difference solution and the experimental resonator was very high. The corresponding variational formulation did not give quite as good results, however, at least for the situation where the trial field became a poorer approximation of the true field. This situation is not unexpected in that it is the nature of a variational formula to establish an upper or lower bound on the parameter which is being expressed.

Comparison of quality factor data for the two approximate techniques and the laboratory data was also made. The finite difference result indicated that the quality factor for the example resonator would be relatively insensitive to changes in the particular resonator structure. The variational formula result for the same resonator indicated that the Q should decrease as the size of the cutoff waveguide sections was increased. This latter result is biased, however, by the fact that the variational calculation of the resonant frequency predicted a somewhat

lower value than was experienced in the laboratory. The corresponding laboratory data indicated the decrease of quality factor as the cutoff waveguide dimension was increased. Uncertainty in the characterization of the resistance, roughness, and porosity of the wall material in the laboratory resonator prevented the absolute comparison of this data with the analytical results.

VII. LITERATURE CITED

1. Adler, R. B., L. J. Chu, and R. M. Fano. Electromagnetic energy transmission and radiation. New York, N.Y., John Wiley and Sons, Inc. 1960.
2. Beaubain, M. J. and A. Wexler. An accurate finite-difference method for higher order waveguide modes. IEEE Transactions on Microwave Theory and Techniques MTT-16, Number 12: 1007-1017. 1968.
3. Beaubain, M. J. and A. Wexler. Unequal-arm finite-difference operators in the positive-definite successive over-relaxation algorithm. IEEE Transactions on Microwave Theory and Techniques MTT-18, Number 12: 1132-1149. 1970.
4. Berk, A. D. Variational principles for electromagnetic resonators and waveguides. IEEE Transactions on Antennas and Propagation AP-4, Number 2: 104-110. 1956.
5. Brown, R. G., R. A. Sharpe, and W. L. Hughes. Lines, waves, and antennas. New York, N.Y., the Ronald Press Company. 1961.
6. Bryant, G. H. Propagation in corrugated waveguides. IEEE Proceedings 116, Number 2: 203-213. 1969.
7. Carre, B. A. The determination of the optimum accelerating factor for successive overrelaxation. Computer Journal 4, Number 1: 73. 1961.
8. Davies, J. B. and C. A. Muilwyk. Numerical solution of uniform hollow waveguides with boundaries of arbitrary shape. IEEE Proceedings 113, Number 2: 277-284. 1966.
9. Finkbeiner, D. T. Matrices and linear transformations. San Francisco, Calif., W. H. Freeman and Company. 1960.
10. Forsythe, G. E. and W. R. Wasow. Finite-difference methods for partial differential equations. New York, N.Y., John Wiley and Sons, Inc. 1960.
11. Gent, A. W. The attenuation and propagation factor of spaced-disc circular waveguide. IEEE Proceedings 106, Number 1: 37-46. 1959.
12. Ginzton, E. L. Microwave measurements. New York, N.Y., McGraw-Hill Book Company, Inc. 1957.
13. Harrington, R. F. Time-harmonic electromagnetic fields. 1st ed. New York, N.Y., McGraw-Hill Book Company, Inc. 1961.

14. Harrington, R. F. Matrix methods for field problems. IEEE Proceedings 55, Number 2: 136-148. 1967.
15. Harrington, R. F. Field computation by moment methods. New York, N.Y., The Macmillan Company. 1968.
16. Hildebrand, F. B. Methods of applied mathematics. Englewood Cliffs, N.J., Prentice-Hall, Inc. 1952.
17. Jahnke, E. and F. Emde. Tables of functions. 4th ed. New York, N.Y., Dover Publications. 1945.
18. Lending, R. D. New criteria for microwave component surfaces. National Electronics Conference Proceedings 11: 391-401. 1955.
19. Marcatili, E. A. Heat loss in grooved metallic surface. IEEE Proceedings 45: 1134. 1957.
20. Matthaei, G. L. and D. B. Weller. Circular TE_{011} -mode, trapped-mode band-pass filters. IEEE Transactions on Microwave Theory and Techniques MTT-13, Number 5: 581-589. 1965.
21. Moreno, T. Microwave transmission design data. New York, N.Y., Dover Publications. 1948.
22. Morrison, J. A. Heat loss of circular electric waves in helix waveguides. IRE Transaction on Microwave Theory and Techniques MTT-6: 173. 1958.
23. Morton, D. M. A tunable trapped-mode resonator. Unpublished M.S. thesis. Ames, Iowa, Library, Iowa State University of Science and Technology. 1968.
24. Post, R. E., A. G. Potter, and V. V. Risser. A "trapped-mode" resonator for microwave filter applications. National Electronics Conference Proceedings 22: 31-35. 1966.
25. Potter, A. G. A periodic type of microwave sampling cavity. Unpublished Ph.D. thesis. Ames, Iowa, Library, Iowa State University of Science and Technology. 1966.
26. Ramo, S., J. R. Whinnery, and T. Van Duzer. Fields and waves in communication electronics. New York, N.Y., John Wiley and Sons, Inc. 1965.
27. Risser, V. V. A narrow-band band-pass microwave filter using trapped-mode resonator cavities. Unpublished M.S. thesis. Ames, Iowa, Library, Iowa State University of Science and Technology. 1967.

28. Rumsey, V. H. Reaction concept in electromagnetic theory. *Physical Review* 94, Number 6: 1483-1491. 1954.
29. Schiffman, B. M., G. L. Matthaei, and L. Young. A rectangular-waveguide filter using trapped-mode resonators. *IEEE Transactions on Microwave Theory and Techniques* MTT-13, Number 5: 575-580. 1965.
30. United States National Bureau of Standards. Handbook of mathematical functions. United States National Bureau of Standards Applied Mathematics Series 55. 1964.
31. Vetter, V. M. and M. C. Thompson, Jr. An absolute microwave refractometer. *Review of Scientific Instruments* 33: 656-660. 1962.
32. Watkins, D. A. Topics in electromagnetic theory. New York, N.Y., John Wiley and Sons, Inc. 1958.
33. Whiting, K. B. A treatment for boundary singularities in finite difference solutions of Laplace's equation. *IEEE Transactions on Microwave Theory and Techniques* MTT-16, Number 10: 889-891. 1968.

VIII. ACKNOWLEDGMENTS

I wish to express my appreciation to Dr. R. E. Post for the assistance he has given me throughout my graduate program.

I am indebted to Mr. D. P. Passeri for his arranging for my use of Bendix Corporation's frequency counter for the laboratory measurements.

To my many acquaintances who have provided numerous constructive conversations thanks are also due.

Finally, to my wife Johnna, I give special thanks for her help and understanding during the course of my work.

IX. APPENDIX A:

VARIATIONAL FORMULATION EXAMPLE

The purpose of this example is to illustrate the utilization of the variational formula developed in this thesis to analyze the resonator which was tested in the laboratory. It should be noted in passing that the chosen trial field is only one of many possible choices and may or may not be the "best" possible choice. The requirements on the trial field are given in detail in the body of this thesis.

As a trial field take the field within that region which corresponds to the closed resonator volume to be the field for a closed resonator. Namely, for $r \leq a$ (region 1)

$$E_{\phi 1} = \sin(\pi z/d) J_1(3.832r/a). \quad (\text{A.1})$$

In the radial section where $r \geq a$ (region 2), assume

$$E_{\phi 2} = \sum_{n=1}^{\infty} h_{ni} \sin(n\pi(z-z_i)/t) K_1(\kappa_n r) \quad (\text{A.2})$$

where h_{ni} is the amplitude of the n th order mode in the i th radial section ($i = 1$ in the section near the $z = 0$ end of the trapped-mode resonator and $i = 2$ in the section at the $z = d$ end.), $z_1 = 0$, $z_2 = d - t$, t is the spacing of the cutoff radial waveguide sections, and κ is determined from the separation equation for the cutoff region as

$$\kappa_n = \left((n\pi/t)^2 - \omega^2 \mu_0 \epsilon_0 \right)^{1/2}. \quad (\text{A.3})$$

Continuity of tangential magnetic field intensity at $r = a$ gives

$$h_{ni} = \frac{-3.832 J_0(3.832) \frac{2}{\kappa_n a K_0(\kappa_n a)} \frac{nd^2}{\pi n^2 d^2 - t^2}}{\pi n^2 d^2 - t^2} [\sin(\pi z_1/d) - \cos(n\pi) \sin(\pi(z_1 + t)/d)]. \quad (A.4)$$

Using the trial field expressed by Equation A.1 and Equation A.2 as supplemented by Equations A.3 and A.4, the complex value of ω^2 may now be evaluated by use of Equation 3.2.17. Useful relationships which are pertinent to the detailed calculations are given in References 17 and 30. The result is

$$\omega^2 = \frac{i_1 + 2i_2 + (R_s(1+j)/\omega_0 \mu_0) i_3}{i_4} \quad (A.5)$$

where

$$i_1 = d((\pi/d)^2 + (3.832/a)^2)/2 + t \sum_{n=1}^{\infty} k_n^2 [(1 - (K_1/K_0)^2) \omega_0^2 \mu_0 \epsilon_0 + (n\pi/t)^2 (2/\kappa_n a) (K_1/K_0)]$$

$$i_2 = (2t/a) \sum_{n=1}^{\infty} \kappa_n k_n^2 (K_1/K_0)$$

$$i_3 = 2(\pi/d)^2 + ((3.832)^2/a^3) (d-2t+(d/\pi)\sin(2\pi t/d)) + (2\pi/at)^2 \sum_{m=1}^{\infty} \sum_{n=1}^{\infty} mn k_m k_n (1+(-1)^{m+n}).$$

$$\cdot \frac{a}{\kappa_n^2 - \kappa_m^2} \left[\kappa_n \frac{K_1(\kappa_m a)}{K_0(\kappa_m a)} - \kappa_m \frac{K_1(\kappa_n a)}{K_0(\kappa_n a)} \right]$$

and

$$i_4 = d/2 + t \sum_{n=1}^{\infty} k_n^2 (1 + (2/\kappa_n a)(K_1/K_0) - (K_1/K_0)^2)$$

where

$$k_n = \frac{3.832}{\kappa_n a} \frac{2}{\pi} \frac{nd^2}{n^2 d^2 - t^2} \sin(\pi t/d)$$

The term (K_1/K_0) is used to denote $(K_1(\kappa_n a)/K_0(\kappa_n a))$, an expression which is known (23). The term i_3 is of indeterminate form when $m = n$ and may be resolved by use of L'Hospital's rule or by evaluating the appropriate integral for this situation.

The complex resonant frequency squared is now determined for the above choice of trial field and may be evaluated conveniently by means of a digital computer program with the summations truncated at an appropriate upper index.

If the complex angular frequency ω is separated into real and imaginary parts as $\omega = \omega_r + j\omega_i$ then

$$\omega^2 = (\omega_r^2 - \omega_i^2) + j2\omega_r\omega_i = (\omega^2)_r + j(\omega^2)_i. \quad (\text{A.6})$$

For high Q situations (13), $\omega_r \gg \omega_i$ and

$$Q = |(\omega^2)_r / (\omega^2)_i| \quad (\text{A.7})$$

which is the desired result for comparison of quality factor data.

It should be noted that if the trial field becomes the exact solution then Equation A.7 is essentially the same result as would be obtained from the usual perturbation analysis except that the real

part of ω^2 will reflect a change in the resonant frequency which is due to the presence of losses. Also, since ω^2 is stationary (possessing a saddle point at $p = 0$ (13)), the quality factor expressed by Equation A.7 is also stationary.

X. APPENDIX B

CONSTRUCTION OF THE FINITE-DIFFERENCE ANALYSIS PROGRAM

The purpose of this program is to solve Maxwell's equations for a linear, homogeneous, source-free region

$$\underline{\nabla} \times \underline{E} = -\mu \partial \underline{H} / \partial t \quad (\text{B.1a})$$

$$\underline{\nabla} \times \underline{H} = \epsilon \partial \underline{E} / \partial t \quad (\text{B.1b})$$

subject to appropriate boundary conditions on conducting surfaces and to calculate the quality factor corresponding to the field solution. The particular geometry of interest is that described in Section IV-A of this thesis. Time dependence of the form $\exp(j\omega t)$ will be assumed implicitly and suppressed in the usual way. Thus Equations B.1 become

$$\underline{\nabla} \times \underline{E} = -j\omega\mu\underline{H} \quad (\text{B.2a})$$

and

$$\underline{\nabla} \times \underline{H} = j\omega\epsilon\underline{E}. \quad (\text{B.2b})$$

One general approach to solving Equations B.2 which has enjoyed some popularity in both continuous (13) and discrete (2, 3, 8) applications is to postulate a (scalar) potential function which is constrained by either Dirichlet or Neumann boundary conditions (as is dictated by the nature of the electromagnetic field solution desired) and derive \underline{E} and \underline{H} from the potential.

The approach here is somewhat more specific in that the electric field will be the quantity which is to be solved for and the magnetic

field determined from it by use of Equation B.2a. This technique, while somewhat less general, is useful in that less derivatives need to be evaluated to determine the complete electromagnetic field solution than in the method using a potential field.

The magnetic field intensity may be eliminated from Equations B.2 to get

$$\underline{\nabla} \times (\underline{\nabla} \times \underline{E}) = \omega^2 \mu \epsilon \underline{E}. \quad (\text{B.3})$$

If \underline{E} is constrained to have only a ϕ -component (in a right-cylindrical coordinate system r, ϕ, z such as is indicated in Figure 2.3) then Equation B.3 reduces to a scalar partial differential equation. Namely,

$$\frac{\partial^2 E_\phi}{\partial \rho^2} + \frac{1}{\rho} \frac{\partial E_\phi}{\partial \rho} - \frac{E_\phi}{\rho^2} + \frac{\partial^2 E_\phi}{\partial z^2} + \omega^2 \mu \epsilon E_\phi = 0. \quad (\text{B.4})$$

The term $\omega^2 \mu \epsilon$ is identifiable as the eigenvalue and will hereafter be denoted as λ .

If the derivatives are written in a form which is in terms of limits as h and k (used here to denote incremental lengths in the r - and z -coordinate directions, respectively) approach zero and Equation B.4 written in the form $L E_\phi = \lambda E_\phi$, then the problem may be expressed in discrete form. The discrete form of L (denoted L_d) is given by

$$\begin{aligned} L_d E_\phi = & E_\phi(r, z) (2/h^2 + 2/k^2 + 1/r^2) - E_\phi(r+h, z) (1/h^2 + 1/2rh) \\ & - E_\phi(r-h, z) (1/h^2 - 1/2rh) - E_\phi(r, z+k) (1/k^2) \\ & - E_\phi(r, z-k) (1/k^2). \end{aligned} \quad (\text{B.5})$$

The desired relaxation formula is determined by equating $L_d E_\phi$ to λE_ϕ and solving for $E_\phi(r, z)$ in terms of the neighboring field values. The result is the relaxation formula R where

$$\begin{aligned}
 E_\phi(r, z) &= R(E_\phi) \\
 &= [E_\phi(r+h, z)(1/h^2 + 1/2rh) \\
 &\quad + E_\phi(r-h, z)(1/h^2 - 1/2rh) \\
 &\quad + E_\phi(r, z+k)(1/k^2) \\
 &\quad + E_\phi(r, z-k)(1/k^2)] / (2/h^2 + 2/k^2 + 1/r^2 - \lambda).
 \end{aligned}
 \tag{B.6}$$

An algorithm which permits unequal length distances between central and neighboring field values in a given coordinate direction, thereby permitting more arbitrary boundaries is given by Beaubien and Wexler (3).

The application of this formula is to an array of discrete data points which correspond to electric field intensity values within the resonator. The boundary of the resonator is described on a surface of constant angular variable ϕ with the values of (tangential) electric field at conductors being zero. The boundary condition in the cutoff radial waveguide for large values of the radial dimension r is approximated by forcing $E_\phi(r=4a, z)$ equal to zero. This is not an unfair approximation in that it reasonably represents the behavior of evanescent fields there.

Reduction of storage space is achieved by forcing symmetry about $z = d/2$. Further reduction is achieved by noting that continuity of

tangential electric field intensity and the lack of ϕ -dependence in the field forces E_ϕ to be zero at $r = 0$. Thus only the section for $0 \leq r \leq 4a$, $0 \leq z \leq d/2$ is considered.

Equation B.6 is applied sequentially to each of the internal points (with $E_\phi(r, d/2 + k)$ set equal to $E_\phi(r, d/2 - k)$) several times with a guessed value for λ . Then, a new value for λ is estimated by using a discrete form of the Rayleigh quotient. Namely,

$$\lambda = - \frac{\sum E_\phi L_d E_\phi}{\sum E_\phi^2} \quad (\text{B.7})$$

where \sum implies summation over all of the field points. Equation B.6 is again applied repeatedly as above until λ converges to within some predetermined tolerance.

The convergence of λ will be hastened somewhat if some acceleration is used. The form of the accelerated relaxation formula is

$$E_\phi(r, z) = \beta R(E_\phi) + (1 - \beta) E_\phi(r, z). \quad (\text{B.8})$$

$E_\phi(r, z)$ on the left side of this equation is interpreted as being the new value being found by the relaxation whereas on the right side it is interpreted as being the value which existed before the application of the accelerated relaxation formula. The accelerating factor β may assume values between 0 and 2. A value of 0 gives total deceleration (no change in E), a value of 1 gives no acceleration (compare Equation B.8 with $\beta = 1$ to Equation B.6), and a value of 2 gives total acceleration (unstable). Carre (7) gives a method for finding the optimum value of the accelerating factor, although the method used for this example

was to simply pick a value. Generally, the value used was in the range of 1.5 to 1.8.

After the convergence of λ is ascertained, the field is relaxed (i.e., Equation B.8 is applied to the array of points) several times with $\beta = 1.0$ in order to insure the convergence of the field values. It should be noted that the eigenvalue converges somewhat faster than does the field in that the Rayleigh quotient is a stationary form. The procedure just described is similar to that of Davies and Muilwyk (8).

Because the introduction of the reentrant corner at the junction of the cutoff radial waveguide and the cylindrical surface of the resonator generates a situation wherein high conduction current may exist (and hence locally high losses), the electric field in that region was expanded using the method of Whiting (33) in an effort to achieve good accuracy there. This method uses a cylindrical modal expansion in the vicinity of a reentrant corner. Whiting's work is for the solution of Laplace's equation although comparison of his expansion with the continuous solution for the electromagnetic field in the vicinity of a corner as given by Harrington (13) shows that the same technique is valid for the solution of the Helmholtz equation being considered here. There is one approximation made here in that the expansion is strictly applied about a straight-line axis but the geometry used here is such that the expansion is made about a curved line. The approximation is justified on the basis that the radius of the region over which the expansion is used is kept somewhat smaller than the radius of curvature of the closed resonator boundary.

This modal expansion is used both during the relaxation process (in order to achieve accuracy without the slow execution penalty resulting from a very fine mesh) and in the calculation of the energy storage and losses in the vicinity of the reentrant corner. These latter calculations are facilitated by using Equation B.2a on each of the modal expansion coefficients with the normalization that $-j\omega\mu = 1$. This normalization results in no loss of generality in that the same normalization is used for the finite difference calculations.

At points away from the reentrant corner, a finite difference form of Equation B.2a is used to calculate the r- and z-directed components of the magnetic field intensity. The calculation is implemented in such a way that the magnitude squared of the magnetic field is calculated and stored in an array which overlaps that used to store the electric field intensity array. Thus only a small amount of additional storage area in the computer is required.

In order to provide a facility to permit easy examination of computer output of the electric or magnetic field array values and to provide information for the evaluation of quality factor data, a subroutine for normalization of the arrays involved was included. The subroutine will normalize either the electric or magnetic field squared arrays with respect to either a supplied normalization factor or with respect to the largest element in the array to be normalized.

Finally the quality factor is determined by performing summations of the magnetic field intensity squared array to provide results which are approximations of the surface and volume integrations which are

required to evaluate an appropriate expression for the quality factor such as that given by Equation 2.2.6.

A listing of the specific main program and various subroutines used in the finite difference analysis of the example resonator and a brief description of the usage of each is given in Appendix C.

XI. APPENDIX C:

FINITE-DIFFERENCE ANALYSIS PROGRAM

The Fortran program listed on the following pages was compiled under the "H" option Fortran compiler at the Iowa State University Computation Center. By the use of overlays at the linkage editor step of the program execution, the listed program will run in 128K bytes of main core storage, providing as much as the equivalent of 101 x 101 field points in the constant ϕ section of the closed cylindrical resonator geometry.

C		MAIN
C	PROGRAM MAIN	MAIN
C		MAIN
C	PROGRAM MAIN IS THE PRIMARY CALLING PROGRAM FOR THE FINITE	MAIN
C	DIFFERENCE ANALYSIS OF THE EXAMPLE TRAPPED MODE RESONATOR. ITS	MAIN
C	PURPOSE IS TO CALL THE SUBROUTINES WHICH EXECUTE THE ANALYSIS.	MAIN
C	THE PURPOSE OF THIS ORGANIZATION IS TO PERMIT RUNNING THE	MAIN
C	COMPILED PROGRAM IN 128K BYTES OF MEMORY BY USE OF OVERLAYS AT	MAIN
C	THE LINKAGE EDITOR STEP. THE OBJECT DECKS WERE COMPILED USING	MAIN
C	H- LEVEL FORTRAN ON THE I.S.U. 360/65 (IBM) COMPUTER.	MAIN
C		MAIN
C	SUBROUTINES USED:	MAIN
C		MAIN
C	ONE	MAIN
C	TWO	MAIN
C		MAIN
C		MAIN
C	CALL ONE(A,D,RC,IO,M,KMAX,AFK,ICSTRT,ICEND,ICSTEP,KMAX1,TOL,	MAIN
5	1 KCONV,AF,DM,U,TERM,DEE,NSTOP)	MAIN
	CALL TWO(A,D,RC,IO,M,KMAX,AFK,ICSTRT,ICEND,ICSTEP,KMAX1,TOL,	MAIN
	1 KCONV,AF,DM,U,TERM,DEE)	MAIN
	IF(NSTOP.NE.0) GO TO 5	MAIN
	STOP	MAIN
	END	MAIN

C
C SUBROUTINE ONE(A,D,IO,L,KMAX,AFK,ICSTRT,ICEND,ICSTEP,KMAX1,TOL,
C KCONV,AF,DM,U,TERM,DEE,NSTOP) ONE
C
C SUBROUTINE ONE SERVES TO INITIATE VARIOUS DATA AND CONSTANTS. ONE
C
C PARAMETERS USED: ONE
C
C A - RADIUS OF RESONATOR IN INCHES ONE
C D - AXIAL LENGTH OF RESONATOR IN INCHES ONE
C RC - SURFACE RESISTANCE COEFFICIENT FOR THE WALL MATERIAL ONE
C BEING CONSIDERED ONE
C IO - ORDER OF THE MESH TO BE USED IN THE FINITE DIFFERENCE ONE
C ARRAY ONE
C L - NUMBER OF TIMES THE RELAXATION ALGORITHM IS TO BE APPLIED ONE
C TO THE ARRAY BEFORE A NEW VALUE FOR THE RAYLEIGH QUOTIENT ONE
C IS EVALUATED ONE
C KMAX - NUMBER OF TIMES THE RAYLEIGH QUOTIENT IS TO BE ONE
C DETERMINED WITH THE ACCELERATION FACTOR EQUAL TO AFK ONE
C AFK - (SEE KMAX, ABOVE) ONE
C ICSTRT,ICEND,ICSTEP - PARAMETERS GIVING THE BEGINNING, ENDING,
C AND INTERMEDIATE INCREMENTS ONE
C (REPECTIVELY) FOR THE LOCATION OF THE ONE
C REENTRANT CORNER OF THE RADIAL SECTION;
C NOTE THAT IF ICSTRT=1, THE FIRST ONE
C CALCULATION CORRESPONDS TO A CLOSED ONE
C RESONATOR ONE
C KMAX1 - NUMBER OF TIMES THAT THE TOLERANCE ON THE EIGENVALUE ONE
C CONVERGENCE MUST BE REPEATED BEFORE THE ACCELERATION ONE
C FACTOR IS CHANGED FROM AFK TO UNITY ONE
C TOL - TOLERANCE ON EIGENVALUE CONVERGENCE ONE
C KCONV - NUMBER OF TIMES THAT THE RAYLEIGH QUOTIENT IS TO BE ONE
C DETERMINED WITH UNITY ACCELERATION FACTOR (AFTER KMAX ONE
C CALCULATIONS OR AFTER THE EIGENVALUE HAS REACHED THE ONE
C DESIRED TOLERANCE ON ITS CONVERGENCE) ONE
C AF - ACCELERATING FACTOR FOR INITIAL RELAXATION ONE
C DM,U,TERM,DEE - VARIABLES INITIALIZED IN THIS SUBROUTINE AND ONE


```
PRINT 303
PRINT 302, ((EXPAND(M,N),N = 1,5),M = 1,5)
PRINT 304
PRINT 302, ((EXPAND(M,N),N = 1,5),M = 1,5)
PRINT 305
PRINT 302, ((ANSWER(M,N),N = 1,5),M = 1,5)
T1 = (PI/BR)**2
TERM = (1. + T1)/(4.*(T1 + .5*D/A))
DEE = FLOAT(IO-1)
RETURN
END
```

```
ONE
ONE
ONE
ONE
ONE
ONE
ONE
ONE
ONE
ONE
```



```

    RI = R(I)**(2.000/3.000)
    AI = A(I)*2.000/3.000
    TWO23 = 2.000**(2.000/3.000)
    DO 1 J = 1,5
    SMALLM(I,J) = (RI**J)*DSIN(AI*OFLOAT(J))
1   BIGM(I,J) = SMALLM(I,J)*(TWO23**J)
    CALL DUMNV (BIGM,5,5,D,L,M)
    DO 2 I = 1,5
    DO 2 J = 1,5
    PROD(I,J) = 0.000
    DO 2 K = 1,5
2   PROD(I,J) = PROD(I,J) + SMALLM(I,K)*BIGM(K,J)
    DO 3 I = 1,5
    DO 3 J = 1,5
    EXPAND(I,J) = SNGL(BIGM(I,J))
3   EMM(I,J) = SNGL(PROD(I,J))
    RETURN
    END

```

```

GEOM
GEOM
GEOM
GEOM
GEOM
GEOM
GEOM
GEOM
GEOM
GEOM
GEOM
GEOM
GEOM
GEOM
GEOM
GEOM
GEOM
GEOM
GEOM

```



```

7001  COSINE(MMN,202-INCR) = CDS( CNST*(PI-A1))
      COSINE(MMN,200+INCR) = CDS( CNST*(PI+A1))
      COSINE(MMN,302-INCR) = CDS( CNST*(PI+A2))
      DO 7003 N = 1,5
      DO 7003 N = 1,M
      MPN = M + N
      MMN = M - N
      C1 = 1.
      C2 = 1.
      IF(MMN.NE.0) C1 = COSINE(MMN,1)
      IF(MMN.NE.0) C2 = COSINE(MMN,301)
      ANS = (C1*(R(1)**MPN) + C2*(R(301)**MPN))/2.
      DO 7004 INDEX = 2,300
      C3 = 1.
      IF(MMN.NE.0) C3 = COSINE(MMN,INDEX)
      ANS = ANS + C3*(R(INDEX)**MPN)
      ANSWER(M,N) = ANS*PI*FLOAT(M*N)/(300.*FLOAT(MPN))
7003  IF(MMN.NE.0) ANSWER(N,M) = ANS
      DO 7005 I = 1,5
      DO 7005 J = 1,5
      RES = R23X**(I+J)/HZ + FLOAT((-1)**(I-J))*(R23Y**(I+J))/HR
      RES = RES*FLOAT(I*J)/(FLOAT(I+J) - 1.5)
7005  RESULT(I,J) = 4.*RES/3.
      RETURN
      END

```

```

NTGRT
NTGRT
NTGRT
NTGRT
NTGRT
NTGRT
NTGRT
NTGRT
NTGRT
NTGRT
NTGRT
NTGRT
NTGRT
NTGRT
NTGRT
NTGRT
NTGRT
NTGRT
NTGRT
NTGRT
NTGRT
NTGRT
NTGRT
NTGRT
NTGRT
NTGRT
NTGRT
NTGRT
NTGRT
NTGRT
NTGRT
NTGRT
NTGRT
NTGRT
NTGRT
NTGRT
NTGRT
NTGRT
NTGRT
NTGRT

```

```

C
C SUBROUTINE TWO(A,D,IO,M,KMAX,AFK,ICSTRT,ICEND,ICSTEP,KMAX1,TOL, TWO
C          KCONV,AF,DM,U,TERM,DEE) TWO
C
C SUBROUTINE TWO CALLS THE VARIOUS SUBROUTINES USED IN THE FINITE TWO
C DIFFERENCE SOLUTION AND PUTPUTS THE RESULTS. TWO
C TWO
C PARAMETERS USED: TWO
C TWO
C   A - RADIUS OF RESONATOR IN INCHES TWO
C   D - AXIAL LENGTH OF RESONATOR IN INCHES TWO
C   RC - SURFACE RESISTANCE COEFFICIENT FOR THE WALL MATERIAL TWO
C        BEING CONSIDERED TWO
C   IO - ORDER OF THE MESH TO BE USED IN THE FINITE DIFFERENCE TWO
C        ARRAY TWO
C   M - NUMBER OF TIMES THE RELAXATION ALGORITHM IS TO BE APPLIED TWO
C        TO THE ARRAY BEFORE A NEW VALUE FOR THE RAYLEIGH QUOTIENT TWO
C        IS EVALUATED TWO
C   KMAX -- NUMBER OF TIMES THE RAYLEIGH QUOTIENT IS TO BE TWO
C        DETERMINED WITH THE ACCELERATION FACTOR EQUAL TO AFK TWO
C   AFK - (SEE KMAX, ABOVE) TWO
C   ICSTRT,ICEND,ICSTEP -- PARAMETERS GIVING THE BEGINNING, ENDING, TWO
C        AND INTERMEDIATE INCREMENTS TWO
C        (RESPECTIVELY) FOR THE LOCATION OF THE TWO
C        REENFRANT CORNER OF THE RADIAL SECTION; TWO
C        NOTE THAT IF ICSTRT=1, THE FIRST TWO
C        CALCULATION CORRESPONDS TO A CLOSED TWO
C        RESONATOR TWO
C   KMAX1 - NUMBER OF TIMES THAT THE TOLERANCE ON THE EIGENVALUE TWO
C        CONVERGENCE MUST BE REPEATED BEFORE THE ACCELERATION TWO
C        FACTOR IS CHANGED FROM AFK TO UNITY TWO
C   TOL - TOLERANCE ON EIGENVALUE CONVERGENCE TWO
C   KCONV - NUMBER OF TIMES THAT THE RAYLEIGH QUOTIENT IS TO BE TWO
C        DETERMINED WITH UNITY ACCELERATION FACTOR (AFTER KMAX TWO
C        CALCULATIONS OR AFTER THE EIGENVALUE HAS REACHED THE TWO
C        DESIRED TOLERANCE ON ITS CONVERGENCE TWO
C   AF - ACCELERATING FACTOR FOR INITIAL RELAXATION TWO

```

```

C          DM,U,TERM,DEE - VARIABLES INITIALIZED IN SUBROUTINE ONE AND      TWO
C          CARRIED TO SUBROUTINE TWO.                                     TWO
C
C          SUBROUTINES USED:                                           TWO
C
C          INIT                                                         TWO
C          RELAX                                                         TWO
C          ROLLY                                                         TWO
C          SQUARE                                                         TWO
C          NORM                                                         TWO
C          QUEUE                                                         TWO
C
C          SUBROUTINE TWO(A,D,RC,IO,M,KMAX,AFK,ICSTRT,ICEND,ICSTEP,KMAX1,TOL,TWO
1          KCONV,AF,DM,U,TERM,DEE)                                       TWO
COMMON /PARAM/HR,HZ,XK                                               TWO
201  FORMAT('1DIMENSIONS OF THE RESONATOR BEING CONSIDERED ARE: RADIUSTWO
1  =',F9.5,' INCHES'/T53,'LENGTH =',F9.5,' INCHES'/T53,'CUTOFF GUIDETWO
2  THICKNESS =',F9.5,' INCHES OR',F8.5,' TIMES THE LENGTH.')          TWO
202  FORMAT(' THE SURFACE RESISTANCE OF THE ASSUMED WALL MATERIAL IS EQTWO
1  UAL TO',1PE12.5,' TIMES THE SQUARE ROOT OF THE FREQUENCY IN HERTZ.TWO
2  ')                                                                    TWO
203  FORMAT(' THE ORDER OF THE ARRAY BEING USED IS',I4,'.')          TWO
204  FORMAT(' THE CLOSED CAVITY EIGENVALUE IS',1PE12.5,'.')          TWO
205  FORMAT(' EACH ITERATION BELOW RELAXES THE ARRAY',I3,' TIMES BEFORETWO
1  A NEW VALUE FOR THE RAYLEIGH QUOTIENT IS CALCULATED.')          TWO
206  FORMAT(' THE RESULT OF ITERATION NUMBER',I3,' IS A VALUE OF',1PE12TWO
1  1.5,' FOR THE RAYLEIGH QUOTIENT. THE ACCELERATION FACTOR USED WAS'TWO
2  ,OPF5.2,')                                                         TWO
207  FORMAT(' THE RESULTS OF SUBROUTINE QUEUE ARE: Q=',1PE11.5,', CQ=',TWO
1  1E11.5,', IS=',E11.5,', IV=',E11.5,', CS=',E11.5,', CV=',E11.5,')TWO
208  FORMAT(' THE THEORETICAL CLOSED CAVITY QUALITY FACTOR IS',1PE12.5,TWO
1  '.')                                                                    TWO
209  FORMAT(' THE QUALITY FACTOR FROM FINITE DIFFERENCE DATA FOR THE RETWO
1  SONATOR CONSIDERED IS',1PE12.5,')                                     TWO
210  FORMAT(' THE THEORETICAL CLOSED CAVITY RESONANT FREQUENCY IS',1PE1TWO
1  12.5,' MEGAHERTZ.')                                                 TWO

```

211	FORMAT(' THE RESONANT FREQUENCY FROM FINITE DIFFERENCE DATA FOR THTWO 1E RESONATOR CONSIDERED IS',1PE12.5,' MEGAHERTZ.')	TWO
212	FORMAT(' ')	TWO
213	FORMAT('1')	TWO
	F(X,D) = SQRT(X)*3.E8/(6.283185*D)	TWO
	QF(Q,X,F,R,U) = Q*SQRT(X)*3.E8*U/(R*SQRT(F))	TWO
	DO 1 IC = ICSTRT,ICEND,ICSTEP	TWO
	TEEI = FLOAT(IC-1)/DEE	TWO
	TEE = TEEI*D	TWO
	PRINT 201, A,D,TEE,TEEI	TWO
	PRINT 202, RC	TWO
	PRINT 203, IO	TWO
	CALL INIT(IO)	TWO
	PRINT 204, XK	TWO
	FR = F(XK,DM)	TWO
	QT = QF(TERM,XK,FR,RC,U)	TWO
	PRINT 205, M	TWO
	XKT = 0.	TWO
	IOUT = 0	TWO
	DO 2 K = 1,KMAX	TWO
	CALL RELAX(IO,IC,M,AFK)	TWO
	CALL ROLLY(IO,IC)	TWO
	PRINT 206, K,XK,AFK	TWO
	IF(K.EQ.KMAX) PRINT 212	TWO
	IF(ABS(XK-XKT).LT.TOL) IOUT = IOUT + 1	TWO
	KS = K + 1	TWO
	IF(IOUT.GE.KCONV) GO TO 3	TWO
2	XKT = XK	TWO
3	KF = KS + KMAX1 - 1	TWO
	DO 4 K = KS,KF	TWO
	CALL RELAX(IO,IC,M,AF)	TWO
	CALL ROLLY(IO,IC)	TWO
4	PRINT 206, K,XK,AF	TWO
	PRINT 212	TWO
	CALL SQUARE(IO,IC)	TWO
	CALL NORM(IO,IC,1,XN,0)	TWO
	CALL QUEUE(IO,IC,XN,Q,CQ,XIS,XIV,CS,CV)	TWO

```
FR = FR*1.E-6
PRINT 210, FR
FR = F(XK,DM)
FO = FR*1.E-6
PRINT 211, FO
PRINT 207, Q,CQ,XIS,XIV,CS,CV
QC = QF(Q,XK,FR,RC,U)
PRINT 208, QT
PRINT 209, QC
PRINT 213
RETURN
END
```

```
TWO
TWO
TWO
TWO
TWO
TWO
TWO
TWO
TWO
TWO
```


	IR(4) = IO	RELAX
	IR(5) = JP2	RELAX
	IZ(1) = IC + 2	RELAX
	IZ(2) = IC	RELAX
	IZ(3) = ICM2	RELAX
	IZ(4) = ICM2	RELAX
	IZ(5) = ICM2	RELAX
	DO 2001 K = 1,M	RELAX
	DO 2002 J = 2,JM2	RELAX
	DO 2003 I = 2,IZM	RELAX
2003	A(I,J) = R(A(I,J+1),A(I,J-1),A(I+1,J),A(I-1,J),J,R2,H2L)	RELAX
	1 *AF - (AF - 1.)*A(I,J)	RELAX
	I = IZS	RELAX
2002	A(I,J) = R(A(I,J+1),A(I,J-1),A(I-1,J),A(I-1,J),J,R2,H2L)	RELAX
	1 *AF - (AF - 1.)*A(I,J)	RELAX
	J = JM1	RELAX
	DO 2008 I = 2,IZM	RELAX
	IF(IC.EQ.1) GO TO 2104	RELAX
	IF(I.EQ.(ICM1)) GO TO 2005	RELAX
	IF(I.EQ.IC) GO TO 2006	RELAX
	IF(I.EQ.(ICP1)) GO TO 2007	RELAX
2104	A(I,J) = R(A(I,J+1),A(I,J-1),A(I+1,J),A(I-1,J),J,R2,H2L)	RELAX
	1 *AF - (AF - 1.)*A(I,J)	RELAX
	GO TO 2008	RELAX
2005	A(I,J) = 0.	RELAX
	DO 2012 L = 1,5	RELAX
2012	A(I,J) = A(I,J) + EMM(3,L)*A(IZ(L),IR(L))	RELAX
	GO TO 2008	RELAX
2006	A(I,J) = 0.	RELAX
	DO 2013 L = 1,5	RELAX
2013	A(I,J) = A(I,J) + EMM(2,L)*A(IZ(L),IR(L))	RELAX
	GO TO 2008	RELAX
2007	A(I,J) = 0.	RELAX
	DO 2014 L = 1,5	RELAX
2014	A(I,J) = A(I,J) + EMM(1,L)*A(IZ(L),IR(L))	RELAX
2008	CONTINUE	RELAX
	I = IZS	RELAX

	A(I,J) = R(A(I,J+1),A(I,J-1),A(I-1,J),A(I-1,J),J,R2,H2L)	RELAX
1	*AF - (AF - 1.)*A(I,J)	RELAX
	IF(IC.EQ.1) GO TO 2001	RELAX
	J = IO	RELAX
	DO 2009 I = 2,ICM2	RELAX
2009	A(I,J) = R(A(I,J+1),A(I,J-1),A(I+1,J),A(I-1,J),J,R2,H2L)	RELAX
1	*AF - (AF - 1.)*A(I,J)	RELAX
	I = ICM1	RELAX
	A(I,J) = 0.	RELAX
	DO 2015 L = 1,5	RELAX
2015	A(I,J) = A(I,J) + EMM(4,L)*A(IZ(L),IR(L))	RELAX
	J = JP1	RELAX
	DO 2010 I = 2,ICM2	RELAX
2010	A(I,J) = R(A(I,J+1),A(I,J-1),A(I+1,J),A(I-1,J),J,R2,H2L)	RELAX
1	*AF - (AF - 1.)*A(I,J)	RELAX
	I = ICM1	RELAX
	A(I,J) = 0.	RELAX
	DO 2016 L = 1,5	RELAX
2016	A(I,J) = A(I,J) + EMM(5,L)*A(IZ(L),IR(L))	RELAX
	DO 2011 J = JP2,JR	RELAX
	DO 2011 I = 2,ICM1	RELAX
2011	A(I,J) = R(A(I,J+1),A(I,J-1),A(I+1,J),A(I-1,J),J,R2,H2L)	RELAX
1	*AF - (AF - 1.)*A(I,J)	RELAX
2001	CONTINUE	RELAX
	IF(IC.EQ.1) RETURN	RELAX
	DO 2017 L = 1,5	RELAX
2017	C(L) = 0.	RELAX
	DO 2018 K = 1,5	RELAX
	DO 2018 L = 1,5	RELAX
2018	C(K) = + EXPAND(K,L)*A(IZ(L),IR(L))	RELAX
	RETURN	RELAX
	END	RELAX


```
3003 RQD = RQD + A(I,J)*A(I,J)
3004 XK = RQN/(RQD*HR*HR)
      RETURN
      END
```

```
ROLLY
ROLLY
ROLLY
ROLLY
```

C		SQUARE
C	SUBROUTINE SQUARE(IO,IC)	SQUARE
C		SQUARE
C	SUBROUTINE SQUARE CALCULATES THE SQUARED MAGNITUDE OF THE	SQUARE
C	MAGNETIC FIELD FROM THE ELECTRIC FIELD, LEAVING THE RESULT IN	SQUARE
C	APPROXIMATELY THE SAME ARRAY AS WAS THE ORIGINAL DATA.	SQUARE
C		SQUARE
C	PARAMETERS USED:	SQUARE
C		SQUARE
C	IO - ORDER OF THE ARRAY	SQUARE
C	IC - LOCATION OF REENTRANT CORNER.	SQUARE
C		SQUARE
C	SUBROUTINE SQUARE(IO,IC)	SQUARE
	COMMON /FIELD/H2(51,402)/PARAM/HR,HZ,XK	SQUARE
	DIMENSION E(51,401)	SQUARE
	EQUIVALENCE (H2(1,2),E(1,1))	SQUARE
	HSQ(V,W,X,Y,Z,J,R) = ((V*FLOAT(J-1)*(1./(FLOAT(J)-1.5)	SQUARE
1	-1./(FLOAT(J)-0.5))+W*FLOAT(J)/(FLOAT(J)-0.5)	SQUARE
2	-X*FLOAT(J-2)/(FLOAT(J)-1.5)**2)	SQUARE
3	+R*((Y-Z)**2)	SQUARE
	R = (HR/HZ)**2	SQUARE
	JA = IO + 1	SQUARE
	IZ = JA/2	SQUARE
	IZM = IZ - 1	SQUARE
	IA = IO - 1	SQUARE
	JR = 4*IA	SQUARE
	J = 1	SQUARE
	DO 5001 I = 1,IZ	SQUARE
5001	H2(I,J) = HSQ(0.,E(I,2),0.,0.,0.,2,R)*9.	SQUARE
	DO 5002 J = 2,IA	SQUARE
	I = 1	SQUARE
	H2(I,J) = HSQ(0.,0.,0.,E(I+1,J),-E(I+1,J),J,R)	SQUARE
	DO 5003 I = 2,IZM	SQUARE
5003	H2(I,J) = HSQ(E(I,J),E(I,J+1),E(I,J-1),E(I+1,J),E(I-1,J),J,R)	SQUARE
	I = IZ	SQUARE
5002	H2(I,J) = HSQ(E(I,J),E(I,J+1),E(I,J-1),E(I-1,J),E(I-1,J),J,R)	SQUARE

C		NORM
C	SUBROUTINE NORM(IO,IC,KEY,XN,KEY2)	NORM
C		NORM
C	SUBROUTINE NORM IS A UTILITY ROUTINE WHICH PERMITS NORMALIZATION	NORM
C	OF EITHER THE ELECTRIC FIELD OR MAGNETIC FIELD SQUARED ARRAYS BY	NORM
C	EITHER A SUPPLIED FACTOR OR BY THE LARGEST ELEMENT IN THE	NORM
C	SUPPLIED ARRAY.	NORM
C		NORM
C	PARAMETERS USED:	NORM
C		NORM
C	IO - ORDER OF ARRAY	NORM
C	IC - LOCATION OF REENTRANT CORNER	NORM
C	KEY - SET TO 0 FOR ELECTRIC FIELD	NORM
C	SET TO 1 FOR MAGNETIC FIELD SQUARED	NORM
C	XN - NORMALIZATION FACTOR (SEE KEY2)	NORM
C	KEY2 - IF 0, SELECT LARGEST ELEMENT OF SUPPLIED ARRAY FOR XN	NORM
C	IF 1, USE VALUE SUPPLIED FOR XN.	NORM
C		NORM
C		NORM
C	SUBROUTINE NORM(IO,IC,KEY,XN,KEY2)	NORM
	COMMON /FIELD/H2(51,402)	NORM
	DIMENSION A(51,401)	NORM
	EQUIVALENCE (H2(1,2),A(1,1))	NORM
	IZ = (IO+1)/2	NORM
	JEND = 4*IO-3	NORM
	IF(IC.EQ.1) JEND = IO	NORM
	IF(KEY.EQ.0) GO TO 4000	NORM
	DO 4101 I = 1,IZ	NORM
	DO 4101 J = 1,JEND	NORM
4101	A(I,JEND - J + 1) = H2(I,JEND - J + 1)	NORM
4000	IF(KEY2.EQ.1) GO TO 4301	NORM
	XN = 0.	NORM
	DO 4001 J = 1,JEND	NORM
	IEND = IZ	NORM
	IF(J.GT.IO) IEND = IC	NORM
	DO 4001 I = 1,IEND	NORM
4001	IF(ABS(A(I,J)).GT.XN) XN = ABS(A(I,J))	NORM

4301	DO 4002 J = 1,JEND	NORM
	IEND = IZ	NORM
	IF(J.GT.IC) IEND = IC	NORM
	DO 4002 I = 1,IEND	NORM
4002	A(I,J) = A(I,J)/XN	NORM
	IF(KEY.EQ.0) RETURN	NORM
	DO 4201 I = 1,IZ	NORM
	DO 4201 J = 1,JEND	NORM
4201	H2(I,J) = A(I,J)	NORM
	RETURN	NORM
	END	NORM

C
C SUBROUTINE QUEUE(IO,IC,XN,QCALC,CQ,SS,SV,AYES,AYEV) QUEUE
C QUEUE
C SUBROUTINE QUEUE CALCULATES FROM THE MAGNETIC FIELD SQUARED QUEUE
C ARRAY THE SUMS WHICH CORRESPOND TO THE INTEGRALS OF THE QUEUE
C MAGNETIC FIELD SQUARED OVER THE VOLUME AND SURFACE OF THE QUEUE
C RESONATOR BEING CONSIDERED. QUEUE
C QUEUE
C PARAMETERS USED: QUEUE
C QUEUE
C IO - ORDER OF THE ARRAY QUEUE
C IC - LOCATION OF REENTRANT CORNER QUEUE
C XN - NORMALIZATION FACTOR USED PREVIOUSLY ON THE ARRAY QUEUE
C QCALC -- RESULTING RATIO OF VOLUME TO SURFACE SUMS QUEUE
C CQ - RATIO CORRESPONDING TO QCALC IN THE IMMEDIATE VICINITY QUEUE
C OF THE REENTRANT CORNER QUEUE
C SS - SURFACE SUM QUEUE
C SV - VOLUME SUM QUEUE
C AYES - TERM CORRESPONDING TO SS AT THE CORNER QUEUE
C AYEV - TERM CORRESPONDING TO SV AT THE CORNER. QUEUE
C QUEUE
C
C SUBROUTINE QUEUE(IO,IC,XN,QCALC,CQ,SS,SV,AYES,AYEV) QUEUE
COMMON /FIELD/A(51,402)/PARAM/HR,HZ,XK QUEUE
COMMON /CORNER/EMM(5,5),EXPAND(5,5),C(5),RESULT(5,5),ANSWER(5,5) QUEUE
DOUBLE PRECISION SVOL,SSURF,H3,VR,VOLUME,VOL,H2PI,A0,A1,A31,A121 QUEUE
DOUBLE PRECISION PI,ADUB,DFLOAT,DBLE,HR2,HZ2,AREA,AA,SP,SC,T,U,V QUEUE
SVOL = 0.D00 QUEUE
PI = 3.1415926535897932D00 QUEUE
HR2 = DBLE(HR) QUEUE
HZ2 = DBLE(HZ) QUEUE
JR = 4*10⁻³ QUEUE
JPA = IO+1 QUEUE
IZ = JPA/2 QUEUE
IOM1 = IO - 1 QUEUE
T = 2.000*DFLOAT(IOM1) QUEUE
U = (DFLOAT(IOM1)-0.25D00)/2.D00 QUEUE

```

V = (DFLOAT(JR-1) - .25D00)/2.000
JEND = JR
IF(IC.EQ.1) JEND = IO
DO 6001 J = 1,JEND
  IF(J.EQ.1) VOLUME = 0.125D00
  IF(J.GT.1.AND.J.LT.JEND) VOLUME = DFLOAT(J-1)
  IF(J.EQ.JEND) VOLUME = (DFLOAT(J-1) - .25D00)/2.000
  IEND = IZ
  IF(J.GT.IO) IEND = IC
  DO 6001 I = 1,IEND
    VOL = VOLUME
    IF(I.EQ.1.OR.I.EQ.IEND) VOL = VOLUME/2.000
    IF(IC.EQ.1) GO TO 6001
    IF(J.EQ.IO.AND.I.EQ.IC) VOL = 0.000
    IF(J.EQ.ID.AND.I.GT.IC) VOL = U
    SVOL = SVOL + DBLE(A(I,J))*VOL
    SVOL = SVOL*2.000*PI*HR2*HZ
    SP = 0.000
    SC = 0.000
    DO 6002 J = 1,JEND
      AREA = DFLOAT(J-1)
      IF(J.EQ.1) AREA = 0.125D00
      IF(J.EQ.ID.AND.IC.EQ.1) AREA = U
      SP = SP + DBLE(A(1,J))*AREA
      IF(IC.EQ.1) GO TO 6103
      DO 6003 JI = JPA,JR
        AREA = DFLOAT(JI-1)
        IF(JI.EQ.JR) AREA = V
        SP = SP + DBLE(A(IC,JI))*AREA
        SSURF = SP*2.000*PI*HR2*HR2
        ICPI = IC + 1
        IF(IC.EQ.1) ICPI = 1
        DO 6004 I = ICPI,IZ
          AREA = 1.000
          IF(I.EQ.1.OR.I.EQ.IZ) AREA = .5000
          SC = SC + DBLE(A(I,IO))*AREA
          IF(IC.EQ.1) GO TO 6104

```

```

QUEUE
QUEUE
QUEUE
QUEUE
QUEUE
QUEUE
QUEUE
QUEUE
QUEUE
QUEUE
QUEUE
QUEUE
QUEUE
QUEUE
QUEUE
QUEUE
QUEUE
QUEUE
QUEUE
QUEUE
QUEUE
QUEUE
QUEUE
QUEUE
QUEUE
QUEUE
QUEUE
QUEUE

```

```

ICM1 = IC - 1
DO 6105 I = 1, ICM1
AREA = 4.000
IF(I.EQ.1.OR.I.EQ.ICM1) AREA = 2.000
SC = SC + DBLE(A(I, J)) * AREA
SSURF = SSURF + SC * T * PI * HR2 * HZ2
6104  AYES = 0.
        AYEV = 0.
        IF(IC.EQ.1) GO TO 6007
        DO 6005 M = 1, 5
        DO 6005 N = 1, 5
        AYES = AYES + C(M) * C(N) * RESULT(M, N)
        AYEV = AYEV + C(M) * C(N) * ANSWER(M, N)
6005  AYES = AYES * T * PI * HR / XN
        AYEV = AYEV * T * PI * HR / XN
6007  SV = SNGL(SVOL) + AYEV
        SS = SNGL(SSURF) + AYES
        QCALC = SV / SS
        CQ = 0.
        IF(ABS(AYES) < .1E-20) RETURN
        IF(IC.NE.1) CQ = AYEV / AYES
        RETURN
END

```

```

QUEUE
QUEUE
QUEUE
QUEUE
QUEUE
QUEUE
QUEUE
QUEUE
QUEUE
QUEUE
QUEUE
QUEUE
QUEUE
QUEUE
QUEUE
QUEUE
QUEUE
QUEUE
QUEUE
QUEUE
QUEUE
QUEUE

```